Microfludic Culture and Analysis of Endothelial Cells in Relation to Cardiovascular Disease and Cancer Metastasis

by

Jonathan Wanserk Song

A dissertation submitted in partial fulfillment
of the requirements for the degree of
Doctor of Philosophy
(Biomedical Engineering)
in The University of Michigan
2008

Doctoral Committee:

Associate Professor Shuichi Takayama, Chair
Professor Jacques E. Nor
Associate Professor Joseph L. Bull
Assistant Professor Gary D. Luker
Assistant Professor Michael Mayer

DEDICATION

This dissertation is dedicated to my mother and father: Hyun Song and Dr. Jae H. Song.

My mother has positively encouraged me to always

expect nothing but the best from myself.

My father has long been my ambassador to wisdom and advice.

ACKNOWLEDGEMENTS

I would like to gratefully acknowledge my advisor, Dr. Shuichi Takayama, for his continued guidance throughout my graduate career. Dr. Takayama represents to me the model brilliant scientist who continually searches for new challenges, pushes boundaries, and is thoroughly committed to the development of his students. I am very thankful to have been one of his students. I would also like to acknowledge the members of my dissertation committee: Drs. Jacques Nor, Michael Mayer, Joseph Bull, and Gary Luker. Some of them have been my collaborators. Others have been my professor. All of whom along with Dr. Takayama are my role models as scientists.

I would like to graciously acknowledge the people who co-authored publications with me that comprise this dissertation: Dr. Kristy Warner, Dr. Nobuyuki Futai, Wei Gu, Yun Seok Heo, Lourdes Cabrera, Dr. Yi-Chung Tung, Dr. Tommaso Bersano-Begey, Dr. Gary Smith, Dr. Kathy Luker, Ann Walker, Mudit Gupta, and Steve Cavnar. I would also like to thank the staff of the BME department, particularly Mayte Brown. Finally, I would like to thank all the members of the Takayama lab and the friends I have made while here at the University of Michigan. During my graduate studies, I have learned and enjoyed myself more than any other time in my life. The people I have met during my time at Michigan are the reasons why.

TABLE OF CONTENTS

LIST OF FIGURES

ABSTRACT

Endothelial cells comprise the inner lining of the entire circulatory system and are key mediators in many aspects of vascular biology. The interaction of endothelial cells with blood-borne constituents and the mechanical forces due to blood flow regulate a broad range of diseases that originate at the vasculature. The challenges of studying endothelial cell biology *in vivo* is that it is highly invasive to access, experimentally manipulate, and/or observe changes inside of blood vessels. Furthermore, current *in vitro*-based systems do not faithfully recreate the mechanical and chemical cellular environments with the proper length scales seen in physiology. Here we show examples of using the tools of microfluidics and microfabrication in developing perfusion-based *in vitro* systems that mimic the *in vivo* environments of endothelial cells. We describe a novel, reconfigurable micro-pumping and valving system that enables the delivery of a wide range of mechanical shear stress to multiple endothelial cell compartments simultaneously. We also utilized this pumping and valving system to culture endothelial cells under continuous recirculation of sub-microliter amounts of fluid. Finally, we engineered a compartmentalized endothelium to model the intravascular adhesion events of circulating cancer cells with endothelium at metastatic and non-metastatic sites. We determined that the endothelium regulates site-specific adhesion of circulating cancer cells that is independent of the predicted metastatic abilities of the cancer cells. Collectively, these results confirm that microfluidic technology can be used to properly

mimic a broad range of the endothelial cell environments seen in physiology. Furthermore, we establish microfluidics as a platform for the development of systems that have the capabilities of advancing the understanding of endothelial cell biology as it relates to vascular diseases.

CHAPTER I

Introduction

The vascular endothelium is comprised of a monolayer of endothelial cells that lines the interior of blood vessels of the entire circulatory system. Under normal physiology, endothelial cells remain in a quiescent and growth-arrested state which originally perpetuated the notion that they served as a passive boundary between blood and the surrounding organ environment.[1] It is now known that endothelial cells are key mediators in many aspects of vascular biology including atherosclerosis[2, 3], thrombosis[4, 5], vascular tone[6-8], angiogenesis[9, 10], and inflammation[11-13]. In turn, these pathophysiological conditions that originate at the endothelium directly contribute to the progression of many diseases such as heart attack, stoke, high blood pressure, cancer, and arthritis.[1] Therefore, an understanding of the responses of endothelial cells to its physiological environment has a fundamental impact in biology and medicine.

The challenges to studying endothelial cell behavior *in vivo* are due in large part to the very invasive nature of accessing, experimentally manipulating, and/or observing changes in blood vessels.[14] *In vitro*-based systems that mimic either the mechanical[7, 15, 16] or chemical environments[17-19] of endothelial cells have contributed greatly to the understanding of endothelial cell biology. However, these *in vitro*-based systems are typically macroscopic in scale. Therefore, these systems fail to faithfully recreate the

cellular environments representative of the conditions seen *in vivo* in terms of short distances between cells with continuous nutrient supply and waste removal.[20] Microfluidic systems, engineered devices that manipulate small amounts of fluids in channels with dimensions of tens to hundreds of microns[21], offers the potential to improve the current state of the art of *in vitro*-based systems for studying endothelial cells. Microfluidic systems possess the ability to integrate precise fluid actuation[22], formation of independent cellular compartments for parallel experiments[23], and spatial control and delivery of biomolecules,[24] within the central construct of channels on the size scale of small blood vessels such as arterioles or venules.[25]

The objective of this thesis research was to develop microfluidic systems specifically designed to advance the understanding of endothelial cell biology. The common threads among the research presented in this thesis are: 1) microfluidic systems fabricated out of poly(dimethylsiloxane) (or PDMS) using soft lithography[26] and 2) microfluidic culture and analysis of primary human microvascular endothelial cells. Chapter II describes the development of a novel, computer-controlled micro-pumping and valving system that enables the delivery of a wide range of mechanical shear stress to multiple endothelial cell compartments simultaneously. The endothelial cells in this system demonstrate the characteristic response of alignment and elongation to shearing flow[16], a result that had not been previously achieved in a self-contained microfluidic system. The work from Chapter III also utilizes the reconfigurable, computer-controlled micro-pumping and valving system described in Chapter II but instead demonstrates real-time imaging of endothelial cell culture under continuous recirculation of sub-microliter

amounts of fluid. Finally, Chapter IV describes a compartmentalized microfluidic endothelium for evaluating the intravascular adhesion of metastatic breast cancer cells expressing different chemokine receptors onto differentially treated endothelium. We determined that the endothelium regulates site-specific adhesion of circulating cancer cells that is independent of the chemokine receptor expression of the cancer cells.

Collectively, these studies confirm that microfluidic technology can be used to properly mimic a broad range of the endothelial cell environments seen in physiology. Furthermore, the microfluidic systems described in this dissertation are not just miniaturized versions of conventional cell culture techniques. Instead, they proceed beyond the current state of the art of *in vitro*-based systems by allowing for multiple cell culture experiments in parallel, more *in vivo*-like culture conditions, and new insights into the intravascular adhesion steps in cancer metastasis. Therefore, the described work has contributed to establishing microfluidics as a platform for the development of systems that have the capabilities of advancing the understanding of endothelial cell biology as it relates to vascular diseases.

References

1. Ingber, D. E., Vascular Control through Tensegrity-Based Integration of Mechanics and Chemistry. In *Endothelial Biomedicine* 1st ed.; Aird, W. C., Ed. Cambridge University Press: New York, 2008; pp 1786-1792.

2. Libby, P.; Aikawa, M., Stabilization of atherosclerotic plaques: new mechanisms and clinical targets. *Nat Med* **2002,** 8, (11), 1257-62.

3. Ogunrinade, O.; Kameya, G. T.; Truskey, G. A., Effect of fluid shear stress on the permeability of the arterial endothelium. *Ann Biomed Eng* **2002,** 30, (4), 430-46.

4. Gerszten, R. E.; Garcia-Zepeda, E. A.; Lim, Y. C.; Yoshida, M.; Ding, H. A.; Gimbrone, M. A., Jr.; Luster, A. D.; Luscinskas, F. W.; Rosenzweig, A., MCP-1 and IL-8 trigger firm adhesion of monocytes to vascular endothelium under flow conditions. *Nature* **1999,** 398, (6729), 718-23.

5. Smith, M. L.; Olson, T. S.; Ley, K., CXCR2- and E-selectin-induced neutrophil arrest during inflammation in vivo. *J Exp Med* **2004,** 200, (7), 935-9.

6. Bao, X.; Lu, C.; Frangos, J. A., Temporal gradient in shear but not steady shear stress induces PDGF-A and MCP-1 expression in endothelial cells: role of NO, NF kappa B, and egr-1. *Arterioscler Thromb Vasc Biol* **1999,** 19, (4), 996-1003.

7. Blackman, B. R.; Garcia-Cardena, G.; Gimbrone, M. A., Jr., A new in vitro model to evaluate differential responses of endothelial cells to simulated arterial shear stress waveforms. *J Biomech Eng* **2002,** 124, (4), 397-407.

8. Yamamoto, K.; Sokabe, T.; Matsumoto, T.; Yoshimura, K.; Shibata, M.; Ohura, N.; Fukuda, T.; Sato, T.; Sekine, K.; Kato, S.; Isshiki, M.; Fujita, T.; Kobayashi, M.; Kawamura, K.; Masuda, H.; Kamiya, A.; Ando, J., Impaired flow-dependent control of vascular tone and remodeling in P2X4-deficient mice. *Nat Med* **2006,** 12, (1), 133-7.

9. Folkman, J., Tumor angiogenesis: therapeutic implications. *N Engl J Med* **1971,** 285, (21), 1182-6.

10. Willett, C. G.; Boucher, Y.; di Tomaso, E.; Duda, D. G.; Munn, L. L.; Tong, R. T.; Chung, D. C.; Sahani, D. V.; Kalva, S. P.; Kozin, S. V.; Mino, M.; Cohen, K. S.; Scadden, D. T.; Hartford, A. C.; Fischman, A. J.; Clark, J. W.; Ryan, D. P.; Zhu, A. X.; Blaszkowsky, L. S.; Chen, H. X.; Shellito, P. C.; Lauwers, G. Y.; Jain, R. K., Direct evidence that the VEGF-specific antibody bevacizumab has antivascular effects in human rectal cancer. *Nat Med* **2004,** 10, (2), 145-7.

11. Grober, J. S.; Bowen, B. L.; Ebling, H.; Athey, B.; Thompson, C. B.; Fox, D. A.; Stoolman, L. M., Monocyte-endothelial adhesion in chronic rheumatoid arthritis. In situ

detection of selectin and integrin-dependent interactions. *J Clin Invest* **1993,** 91, (6), 2609-19.

12. Low, J.; Kellner, D.; Schuette, W., An automated high capacity data capture and analysis system for the in vitro assessment of leukocyte adhesion under shear-stress conditions. *J Immunol Methods* **1996,** 194, (1), 59-70.

13. Muller, W. A., Leukocyte-endothelial cell interactions in the inflammatory response. *Lab Invest* **2002,** 82, (5), 521-33.

14. Feng, D.; Nagy, J. A.; Dvorak, H. F.; Dvorak, A. M., Ultrastructural studies define soluble macromolecular, particulate, and cellular transendothelial cell pathways in venules, lymphatic vessels, and tumor-associated microvessels in man and animals. *Microscopy Research and Technique* **2002,** 57, (5), 289-326.

15. Lawrence, M. B.; McIntire, L. V.; Eskin, S. G., Effect of flow on polymorphonuclear leukocyte/endothelial cell adhesion. *Blood* **1987,** 70, (5), 1284-90.

16. Helmlinger, G.; Geiger, R. V.; Schreck, S.; Nerem, R. M., EFFECTS OF PULSATILE FLOW ON CULTURED VASCULAR ENDOTHELIAL-CELL MORPHOLOGY. *Journal of Biomechanical Engineering-Transactions of the Asme* **1991,** 113, (2), 123-131.

17. Folkman, J.; Haudenschild, C., Angiogenesis in vitro. *Nature* **1980,** 288, (5791), 551-6.

18. Kubota, Y.; Kleinman, H. K.; Martin, G. R.; Lawley, T. J., Role of laminin and basement membrane in the morphological differentiation of human endothelial cells into capillary-like structures. *J Cell Biol* **1988,** 107, (4), 1589-98.

19. Passaniti, A.; Taylor, R. M.; Pili, R.; Guo, Y.; Long, P. V.; Haney, J. A.; Pauly, R. R.; Grant, D. S.; Martin, G. R., A simple, quantitative method for assessing angiogenesis and antiangiogenic agents using reconstituted basement membrane, heparin, and fibroblast growth factor. *Lab Invest* **1992,** 67, (4), 519-28.

20. Walker, G. M.; Zeringue, H. C.; Beebe, D. J., Microenvironment design considerations for cellular scale studies. *Lab Chip* **2004,** 4, (2), 91-7.

21. Whitesides, G. M., The origins and the future of microfluidics. *Nature* **2006,** 442, (7101), 368-73.

22. Unger, M. A.; Chou, H. P.; Thorsen, T.; Scherer, A.; Quake, S. R., Monolithic microfabricated valves and pumps by multilayer soft lithography. *Science* **2000,** 288, (5463), 113-6.

23. Gu, W.; Zhu, X.; Futai, N.; Cho, B. S.; Takayama, S., Computerized microfluidic cell culture using elastomeric channels and Braille displays. *Proc Natl Acad Sci U S A* **2004,** 101, (45), 15861-6.

24. Takayama, S.; Ostuni, E.; LeDuc, P.; Naruse, K.; Ingber, D. E.; Whitesides, G. M., Subcellular positioning of small molecules. *Nature* **2001,** 411, (6841), 1016.

25. Lipowsky, H. H., Microvascular rheology and hemodynamics. *Microcirculation* **2005,** 12, (1), 5-15.

26. Whitesides, G. M.; Ostuni, E.; Takayama, S.; Jiang, X.; Ingber, D. E., Soft lithography in biology and biochemistry. *Annu Rev Biomed Eng* **2001,** 3, 335-73.

CHAPTER II

Computer-Controlled Microcirculatory Support System for Endothelial Cell Culture and Shearing

Endothelial cells (ECs) lining the inner lumen of blood vessels are continuously subjected to hemodynamic shear stress which is known to modify EC morphology and biological activity. This paper describes a self-contained microcirculatory EC culture system that efficiently studies such effects of shear stress on EC alignment and elongation *in vitro*. The culture system is composed of elastomeric microfluidic cell shearing chambers interfaced with computer-controlled movement of piezoelectric pins on a refreshable Braille display. The flow rate is varied by design of channels that allow for movement of different volumes of fluid per variable-speed pump stroke. The integrated microfluidic valving and pumping system allowed primary EC seeding and differential shearing in multiple compartments to be performed on a single chip. The microfluidic flows caused ECs to align and elongate significantly in the direction of flow according to their exposed levels of shear stress. This system overcomes the small flow rates and inefficiencies of previously described microfluidic and macroscopic systems respectively towards engineering the *in vivo* like environment for the study of EC response to shear stress within a microfluidic setting.

Introduction

Microfluidic systems enable for a high level of fluidic control to create *in vivo* like microenvironments for cell culture.[1-10] Most microfluidic culture systems to date, however, have focused primarily on regulating the chemical environment and not the fluid mechanical environment of cells, such as the exposure of endothelial cells (ECs) to physiological levels of shear stress (5-20 dyn/cm^2).[11] The difficulty is due, at least in part, to the lack of integrated microfluidic pumps that can sustain high enough levels of shear stress in cell culture compatible conditions for the duration of time required (hours to days) to observe cellular effects. Here, we report the use of self-contained, computer-controlled microfluidic cell culture chamber arrays where high-velocity (max of 3 cm/s) pulsatile fluid flows inside high-resistance microchannels generate shear stress levels capable of fluid mechanical regulation of EC phenotypes.

ECs comprise the endothelium or the monolayer of cells lining the inner wall of blood vessels subjected to hemodynamic shear stress *in vivo*. ECs have the property to dynamically sense changes in shear stress levels present in their environment.[12] The responsiveness of ECs to changes in shear stress levels is assessed by modifications in morphology including alignment and elongation in the direction of flow,[13,14] adaptation of cytoskeleton-associated proteins,[15] fluctuations in intracellular calcium concentration involved with cell signaling,[16] secretion of factors necessary for survival,[17] and expression levels of genes.[18] A fundamental question in cardiovascular research is how the mechanical forces associated with shear stress are first sensed and then transduced by ECs into certain diseased states such as thrombosis[19] or atherosclerosis.[20] In order to

address this question, many cardiovascular researchers model or recreate physiological flow conditions *in vitro* with macroscopic systems utilizing external pumping mechanisms, viscometers, and/or fluid reservoirs.[13,14,21] Although these systems produce well-defined fluid flows to relate shear stress levels with a measurable biological response, they are limited due to their consumption of large amounts of reagents, potential for contamination, decreased portability, and inability to perform multiple experiments simultaneously. This system addresses the limitations of existing macroscopic systems by employing a self-contained, re-circulating poly(dimethylsiloxane) (PDMS) microfluidic device with parallel channels interfaced with a refreshable array of piezoelectric pins of a commercially available Braille display.[22] Each piezoelectric pin functions as an actuator for a microfluidic valve when its up-and-down movement is used to deform the elastomeric PDMS microchannels.[23] Fluid is pumped through the microchannels using a variable-speed, 3-pin, peristaltic sequence. The valving capabilities of the microarray of Braille pins enable for one-step seeding of multiple cell shearing compartments that can then be re-circulated simultaneously in parallel but under different cell shearing conditions. The system generates different shear stress levels at the same pumping frequency by varying the size of the contact area of the microchannels where the pins press in which allows for displacement of different volumes of liquid per pump stroke. Flow rates sufficient for EC shearing are produced by maximizing the size of this contact area such that the displacement of fluid is large. This system concurrently addresses the restricted flow rates of microfluidic systems and the inefficiencies of macroscopic systems thereby

opening new windows for evaluating the physiological and biological effects associated with application of shear stress to ECs *in vitro*.

Experimental Section

Device Fabrication. The microfluidic device (Figure II.1a) was fabricated from three layers of poly(dimethylsiloxane) (PDMS) formed from prepolymer (Sylgard 184, Dow Corning) at a ratio of 10:1 base to curing agent. The top layer was formed by replica molding of the prepolymer against relief features machined from brass and steel bars (Figure II.1b) to form fluid reservoirs and cured overnight at 60°C. The middle layer was formed using soft lithography[24] to form a layer with negative relief channel features ~30 μm in height and 300 μm in width. The positive relief features of the mold were composed of SU-8 (Microchem, Newton, MA) formed on a thin glass slide (200 μm thick) using backside diffused-light photolithography.[23] The glass slide was silanized with tridecafluoro-1,1,2,2-tetrahydrooctyl)-1-trichlorosilane (United Chemical Technologies Inc., Bristol, PA). The prepolymer was cured at 60°C overnight and holes were punched in it to connect channel features to the culture media reservoir. The negative relief channel features were sealed against a flat thin membrane layer formed by spin coating prepolymer onto silanized glass slides and cured at 150°C overnight. PDMS cured at 150°C as opposed to 60°C demonstrates more consistent mechanical properties.[25] The three layers were sealed irreversibly by treating with plasma oxygen (SPI Supplies, West Chester, PA) for 30 seconds, pressing the flat surfaces together, and placing in 60°C for 5-10 minutes. Immediately after sealing, sterile phosphate buffered saline (PBS) was

injected to maintain the hydrophilic nature of the channels. Shortly after, the device was sterilized by placing under UV light for ~30 minutes.

Fluid Actuation. A Braille display (DotView DV-1, KGS, Japan) provided a grid (32 x 24) of piezoelectric pins (1.3 mm in diameter) that function as an array of microfluidic valves and pumps. The microfluidic device interfaces with the Braille display by simply holding the device in place such that the channels align with the Braille pins (Figure II.1b) which push upward with a force of 4 cN or approximately $1/100^{th}$ of a pound force (manufacturer's specifications). The Braille pins were controlled with a computer program written in C++ that manipulates the pins to either remain in the up position and act as valves (Figure II.2a) or be components of a 3-pin peristaltic pump that actuates fluid in a pulsatile nature (Figure II.2b). The microfluidic channels were designed such that both low shear stress levels (maximum shear stress ~5 dyn/cm^2 per pump cycle) and high shear stress levels (maximum shear stress ~60 dyn/cm^2 per pump cycle) can be generated within the same loop by changing the volume displacement per pump stroke (Figure II. 2b). Flows at low and high shear levels were actuated by what will be denoted as "small pump" and "large pump" respectively. The average shear stress levels of both the small and large displacement pumps were controlled by changing the frequency of the pumping sequence.

Characterization of Fluid Flows. 6 micron diameter fluorescent (Carnine) polystyrene microspheres Molecular Probes, Eugene, OR) were tracked using a digital CCD camera (Hamamatsu ORCA-ER) and a fluorescence stereomicroscope (Nikon

SMZ1500). Images sequences were acquired at ~15 frames/s to determine the velocity of the microspheres which are representative of the fluid velocity and used to determine the time-varying fluid flow rate *Q(t)*. The Womersley number, α, is a dimensionless parameter used to describe the pulsatile nature of fluid flow in response to an unsteady pressure gradient[26] and is defined as:

$$\alpha = h\sqrt{\frac{\omega}{\nu}} \quad (1)$$

where h is the height of the channel (~30 μm), ω is frequency of pumping, and ν is the kinematic viscosity. For the described microfluidic device, α is small (<<1) and thus the unsteady effects on shear stress levels are negligible. For fully developed, steady channel flow, the shear stress (τ_{cell}) that cells are exposed to is expressed as:

$$\tau_{cell} = \frac{6\mu Q}{h^2 w} \quad (2)$$

where μ is the dynamic viscosity, Q is the fluid flow rate, and w is the width of the channel (~ 300 μm). However, since the pulsatile effects on shear stress are negligible, the time-varying values of shear stress, $\tau_{cell}(t)$, can be determined by replacing Q in (2) with $Q(t)$.[14] The average flow rate and average shear stress levels for the given pump and pumping frequency were determined by taking the time-average of the discrete values of $Q(t)$ and $\tau_{cell}(t)$ respectively over one wavelength multiple times and then performing statistical analysis to determine the average and standard error of measurement (SEM).

General Cell Culture. Human dermal microvascular endothelial cells (HDMECs, Cambrex, East Rutherford, NJ) passage number 7-13 were cultured in endothelial growth medium-2 (EGM-2, Cambrex) in T-75 culture flasks (Corning, Acton, MA) that were placed in a humidified 5% CO_2 cell culture incubator. The HDMECs were collected by washing and detaching with 0.25% Trypsin/EDTA (Invitrogen, Carlsbad, CA). The Trypsin solution was neutralized with 10% FBS in DMEM and spun down with a centrifuge (ThermoForma, Marietta, OH) for 5 min, 4^{o} C, 800 RPM. The supernatant was removed and the pellet was resuspended in EGM-2. The spin and resuspension in EGM-2 were repeated to ensure removal of Trypsin which inhibits cell adhesion during seeding.

Cell Seeding and Microfluidic Cell Culture and Shearing. Prior to cell seeding, fibronectin solution (Invitrogen) at a concentration of 100 μg/ml in PBS was injected along the cell seeding channel to promote cell adhesion. The fibronectin solution was introduced into regions of the microchannels defined by the valves created by the Braille display using two 30 gauge insulin needles, one to vent and one to inject. The fibronectin solution coated the channel surface for 30 minutes at 25^{o}C and then was rinsed by circulating PBS from the reservoir for 30-60 minutes. PBS was then replaced in the reservoir with EGM-2 to rinse the PBS by circulating for 30-60 minutes. Subsequently, the cell solution (~10^{6} cells/ml) was injected into the microchannels in the same manner as the fibronectin solution. After the cells were seeded, the seeding channel was valved at locations to form individual cellular compartments to be circulated with loops that are pumped independently of each other (Figure II.2a). The device and Braille

display were placed in a 37°C/5% CO_2 dry incubator to allow for the cells to attach for 60-90 minutes. After the cells attach, culture media was circulated with the small pump at the desired pumping frequency to sustain the cells for the next 48-72 hours with the culture media in the reservoir being replaced every 24 hours. Once the cells reached the desired level of confluence, the culture media was replaced and remained for the duration of the subsequently described experiment.

Two experiments were conducted to compare the effects of varying levels of shear stress on cell morphology. The first experiment compared two compartments located within the same device with one circulated with the small pump and the other with the large pump and both circulated at the same frequency of 1.0 Hz. Since both compartments were located in the same device, they shared the same culture media. The time-average values of shear stress at a pumping frequency of 1.0 Hz were determined with eq 2 to be <1 dyn/cm^2 for the small pump and ~9 dyn/cm^2 for the large pump. The second experiment compared the changes in cell morphology in three compartments located within the same device that were all circulated with the large pump but at different pumping frequencies of 0.25 Hz, 0.75 Hz, and 2.0 Hz. The time-average shear stress values were determined with eq 2 to be approximately 3 dyn/cm^2 (0.25 Hz), 7 dyn/cm^2 (0.75 Hz), and 12 dyn/cm^2 (2.0 Hz).

Quantification of Cellular Alignment and Elongation. The morphological response of ECs to shear stress was measured with angle of orientation and the Shape Index (*SI*) which are commonly used parameters that quantify the extent that the ECs

align and elongate in the direction of flow respectively. Briefly, the angle of orientation is defined by the angle formed by the cell's major axis and the direction of flow where 0 deg is a cell aligned perfectly with the direction of flow and 90 deg is a cell aligned orthogonal to the direction of flow. The *SI* is a dimensionless measure of the roundness of a cell that is defined as:

$$SI = \frac{4\pi A}{P^2} \quad (3)$$

where A is the area of the cell and P is the perimeter of the cell. The *SI* ranges from 0 to 1 where 0 is a straight line and 1 is a perfect circle. For cells in static culture, the mean angle of orientation is ~45 deg with a large standard of deviation and the mean *SI* value is about 0.8 indicating that the population of cells is randomly oriented and very round in shape.[14] However, since the cells in the described system are cultured in microchannels under flowing conditions with the small pump before they are sheared with the large pump, the typical baseline values for angle of orientation (30-40 deg) and *SI* (0.6-0.7) are slightly less and thus indicates that they are slightly more aligned and less round than cells in static culture conditions.

EC images were obtained using an inverted phase contrast microscope (Nikon TE 300) and a digital CCD camera (Hamamatsu ORCA-ER) at 10X magnification. Images were taken at the onset of circulation with the large pump and every 6-12 hours thereafter. The images were analyzed with Simple PCI imaging software program (Compix Inc. Cranberry Township, PA) to measure the angle of orientation and the *SI* of

individual cells. This data was then exported to an Excel spreadsheet to determine the sample average and the SEM values for angle of orientation and *SI* for each time frame.

Statistics. Statistical differences between experimental groups were evaluated using two-sample Student t-tests at a 95 percent confidence level assuming unequal variances.

Results and Discussion

Characterization of Fluid Flows. The purpose of this study was to recreate pulsatile shear stress levels capable of remodeling ECs within a microfluidic setting. The generation of pulsatile flow is of immense physiological importance because it represents the nature of blood flow in the arterial vasculature that produces shear stress levels modifying EC morphology. Since ECs demonstrate the ability to distinguish between pulsatile versus non-pulsatile flow,[14] in order to be physiologically relevant, the described *in vitro* system must not only generate flow with average shear stress levels seen *in vivo* (5-20 dyn/cm^2)[11] but deliver it in a pulsatile nature as well.

The pulsatile flow was characterized by relating the average flow rate to the pumping frequency (Figure II.2c). For the small pump, the average flow rate increased linearly (R-squared = 0.99) with pumping frequency and the maximum average flow rate achieved was $5.3 \cdot 10^{-3}$ microliters/s at a pumping frequency of 2.0 Hz. The maximum pumping frequency applied for the small pump as well as the large pump was 2.0 Hz because pumping frequencies above 2.0 Hz are not commonly present within the blood

circulation *in vivo*.[27] As seen with the small pump, the average flow rate for the large pump increased linearly with smaller values of pumping frequency. However, unlike the small pump, the average flow rate for the large pump plateaus for pumping frequencies larger than ~0.75 Hz (Figure II.2c) reaching a maximum average flow rate of $4.9 \cdot 10^{-2}$ microliters/s at a pumping frequency of 2.0 Hz. For smaller values of pumping frequencies (<0.75 Hz), the average flow rate for the large pump was ~20 times larger than the average flow rate for the small pump. At a pumping frequency of 2.0 Hz, the average flow rate for the large pump was ~10 times larger than the average flow rate for the small pump exhibiting a significant plateau effect for increased pumping frequency with the large pump.

The plateau effect was only seen with the large pump and indicates reduced efficiency in actuating fluid in the forward direction for pumping frequencies above ~0.75 Hz. This plateau effect is most likely due to one of the steps in the pumping sequence becoming rate-limiting with increased pumping frequency.

EC Morphology Response to Cell Shearing Conditions. The responsiveness of ECs to different levels of shear stress was evaluated in terms of changes in morphology. Figure II.3a is a time-lapse comparison between the changes in EC morphology due to the small pump (average shear stress <1 dyn/cm^2) versus the large pump (average shear stress ~9 dyn/cm^2) both circulated at a pumping frequency of 1.0 Hz. The images suggest that the morphology of the cells circulated by the small pump at 1.0 Hz remain random in orientation and relatively round in shape whereas the morphology of the cells

circulated by the large pump at 1.0 Hz progressively align and elongate in the direction of flow with time. Alignment and elongation were quantified in terms of EC angle of orientation (Figure II.3b) and *SI* (Figure II.3c) respectively. For the small pump, angle of orientation decreased 10 deg (values given for changes in angle of orientation and *SI* are approximate) from T = 0 h and T = 6 h but did not change significantly after T = 6 h ($p>0.05$). The decrease in angle of orientation from T = 0 h to T = 6 h was not expected and is considered a measurement artifact based on results from previous experiments. Thus, for the small pump, neither the angle of orientation nor the shape index (*SI*) for the ECs changed significantly from T = 0 h to T = 24 h ($p>0.05$).

For the large pump, both angle of orientation and *SI* decreased significantly ($p<0.0001$) from T = 0 h to T = 24 h. The ECs cultured with the large pump exhibited a decrease in angle of orientation by 20 deg and a decrease in *SI* by 0.21 from T = 0 to T = 24 h. The percent decrease from T = 0 to T = 24 h for angle of orientation and SI were 57% and 32% respectively. There was also a substantial decrease in the standard of deviation of the angle of orientation from T = 0 h to T = 24 h which is characteristic of EC alignment in the direction of flow.[14] Furthermore, the angle of orientation and the *SI* values were significantly different than the values for the small pump at T = 24 h ($p<0.0001$). In agreement with previous studies, EC elongation occurred more rapidly than alignment under cell shearing conditions (Figure II.3b and II.3c).[28] In addition, the cell density remained steady between 400-550 cells/cm^2 for both experiments for the duration of the experiment demonstrating that cell detachment was not an issue for the given pumping conditions (data not shown).

The morphological response of the ECs validate that this *in vitro* model system is capable of generating shear stress levels sufficient enough to modify EC phenotypes. The average shear stress levels were altered by changing the amount of fluid displacement per pump stroke at a constant pumping frequency. In addition, it is possible to vary the average shear stress levels by changing the pumping frequency while keeping the amount of fluid displacement per pump stroke constant. Figure II.4 shows results from a single chip three-loop experiment where each loop of ECs were exposed to flow generated by large pumps but the average shear stress was varied by changing the pumping frequency. Average shear stress levels ranging from ~2.5 dyn/cm^2 to 12 dyn/cm^2 were generated by varying the pumping frequency between 0.25 and 2 Hz. All flow conditions exhibited the ability to significantly modify EC morphology in terms of alignment and elongation ($p<0.0001$). It has been shown previously that it is the average shear stress that is the primary factor that regulates the relative timing of EC alignment and elongation.[21] The results of the multiple cell shearing experiment support those previous outcomes.

The described microfluidic system has five characteristics that make it advantageous over existing macroscopic systems used to study EC response to shear stress. *(i)* One-step seeding of cells into multiple compartments. *(ii)* Re-circulation of cell culture media from a single reservoir only ~1 ml in volume. *(iii)* Cells and reagents once placed within the device remain there indefinitely. *(iv)* Multiple culture loops whose pulsatile fluid flows are actuated independently of each other. *(v) S*ystem remains

portable enough to be placed entirely within a cell culture incubator. The combination of these characteristics address the limitations of macroscopic systems such as consumption of large amounts of cells and reagents, potential for contamination, decreased portability, and inability to efficiently perform multiple pulsatile flow experiments in parallel. This current device is restricted in its range of average shear stress levels that it can generate (up to ~12 dyn/cm^2) which does not encompass the entire range of average shear stress levels seen physiologically (5-20 dyn/cm^2).[11] The system, however, to our knowledge is the first one of its kind that produces shear stress levels that align and elongate ECs with pulsatile fluid flow and hence demonstrates the ability to create an arterial-like microenvironment within a self-contained, reconfigurable microfluidic device.

Conclusion

We present the foundation for an *in vitro* microfluidic cell culture system that recreates physiological conditions present in the EC environment *in vivo* in terms of shear stress levels and pulsatile flow patterns. Pulsatile flow is essential for this system to be physiologically relevant because ECs have the marked ability to discriminate between pulsatile and non-pulsatile flow.[14] The generation of pulsatile flow was accomplished by integrating the elastomeric channels of the microfluidic device with an array of Braille pin actuators to create a 3-pin peristaltic pump. Previously described microfluidic systems[3,22] are limited in their capacity in generating high enough levels of shear stress necessary for EC remodeling. This system overcomes these limitations by designing the microfluidic channels to maximize the volume displacement per Braille pin actuation. Efficiency not present in macroscopic systems is intrinsic to this design because the microarray of pin actuators coupled with elastomeric channels enables one-step seeding of multiple cell shearing chambers, followed by compartmentalization of the chambers into separate circulation loops, and simultaneous culture of ECs in the different compartments under different shear stress conditions. Furthermore, the flexibility of the design should allow for ready incorporation of additional analytical components. This marks a significant step in creating a fully-integrated microfluidic device capable of providing greater insight into the mechanisms involved with mechanotransduction of signals associated with shear stress that regulate EC phenotype.

Figure II.1. Microfluidic device for EC culture and shearing. (a) Photograph of the device. (b) Three-dimensional schematic depicting the three-layer device fabrication placed on top of a grid of Braille pins. The approximate thickness of the top, middle, and bottom layers are 1 cm, 1 mm, and 100-200 μm respectively. The top layer contains two reservoirs: one to house cell culture media ('culture media reservoir') to be circulated and the other containing water ('evaporation reservoir') to assist in preventing evaporation within the microfluidic channels. The volume of both reservoirs is ~1 ml. The bottom layer serves as a thin membrane that provides the interface between the Braille pins and microfluidic channels of the middle layer.

a

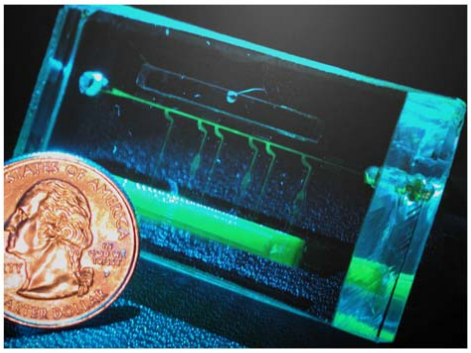

b

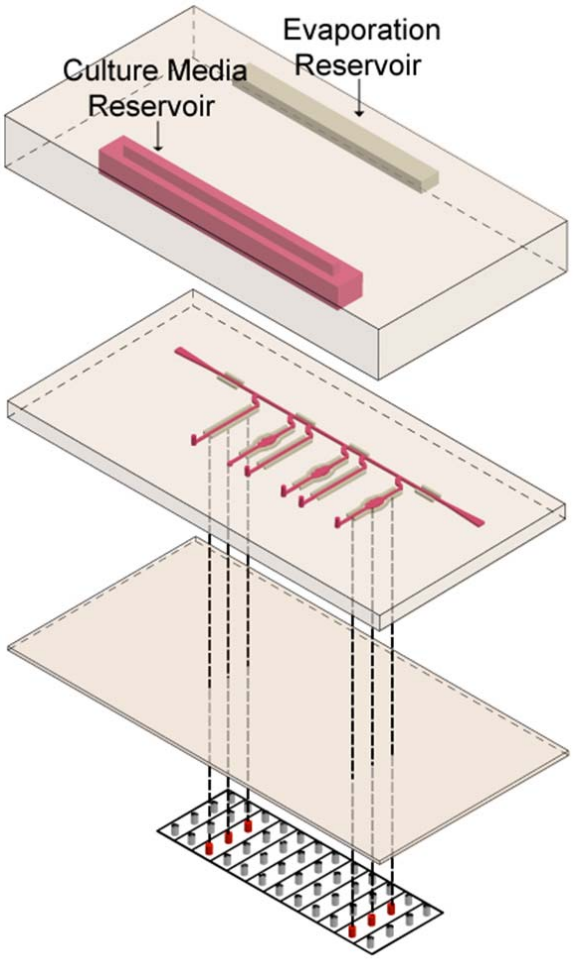

Figure II.2. Demonstration of the microfluidic valves and pumps for cell culture. (a) Close-up of cells attached within an individual cellular compartment. The individual compartments are created by the Braille pins acting as valves which are depicted by the dark circles along the horizontal region of the channel. Each compartment is circulated by flow loops that actuate fluid independently of each other. Fluid in each flow loop can be actuated either clockwise by the small pump (dashed curved line and arrows) or counterclockwise by the large pump (solid curved line and arrows). Cells shown were cultured under cell shearing conditions for 12 h. (b) Step-wise depiction of the peristaltic pumping sequence comparing the small pump and large pump. Fluid is actuated through the channels in a pulsatile nature via a 3-pin, repeating 4-step peristaltic pumping sequence.[22] In this particular pumping sequence, it is Step 2 or the step where the middle pin of the 3-pin pump moves from the down to the up position that drives most of the fluid in the forward direction. The other steps in the pumping sequence prime the pump to maximize volume displacement during Step 2. Increased shear stress levels are generated by the large pump by increasing the area of the channel that is positioned over the middle pin of the 3-pin pump reaching a maximum width equal to approximately the diameter of the Braille pin (1.3 mm). The pair of auxiliary dead-end channels that run parallel to fluidic channels act as void spaces to assist in deformation based actuation due to the Braille pins. These void space channels are of the same height as the fluidic channels due to them being fabricated concurrently during the backside diffused-light lithography process.[23] (c) Comparison of pumping capabilities of small pump and large pump. The average flow rate (microliters/s) for the small pump (■) and the large pump (♦) were plotted against the pumping frequency (Hz). Error bars represent SEM (note: some of the values for SEM are at a value so small that the error bars do not extend beyond the boundary of the shapes at certain data points and are not visible) .

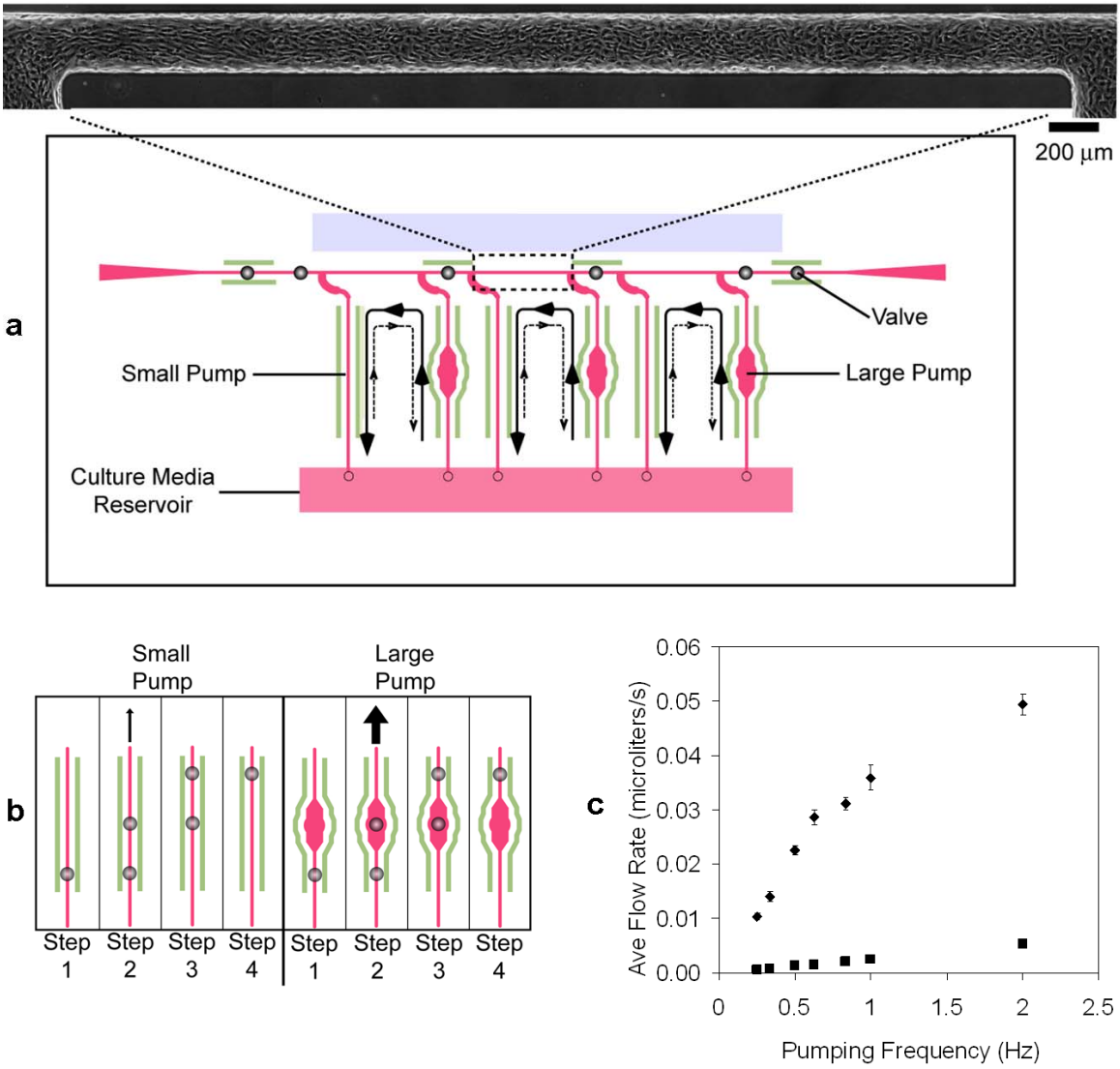
200 µm
a
Valve
Small Pump
Large Pump
Culture Media
Reservoir
b
Small
Pump
Large
Pump
Step 1
Step 2
Step 3
Step 4
Step 1
Step 2
Step 3
Step 4
c
Ave Flow Rate (microliters/s)
0.06
0.05
0.04
0.03
0.02
0.01
0.00
0
0.5
1
1.5
2
2.5
Pumping Frequency (Hz)

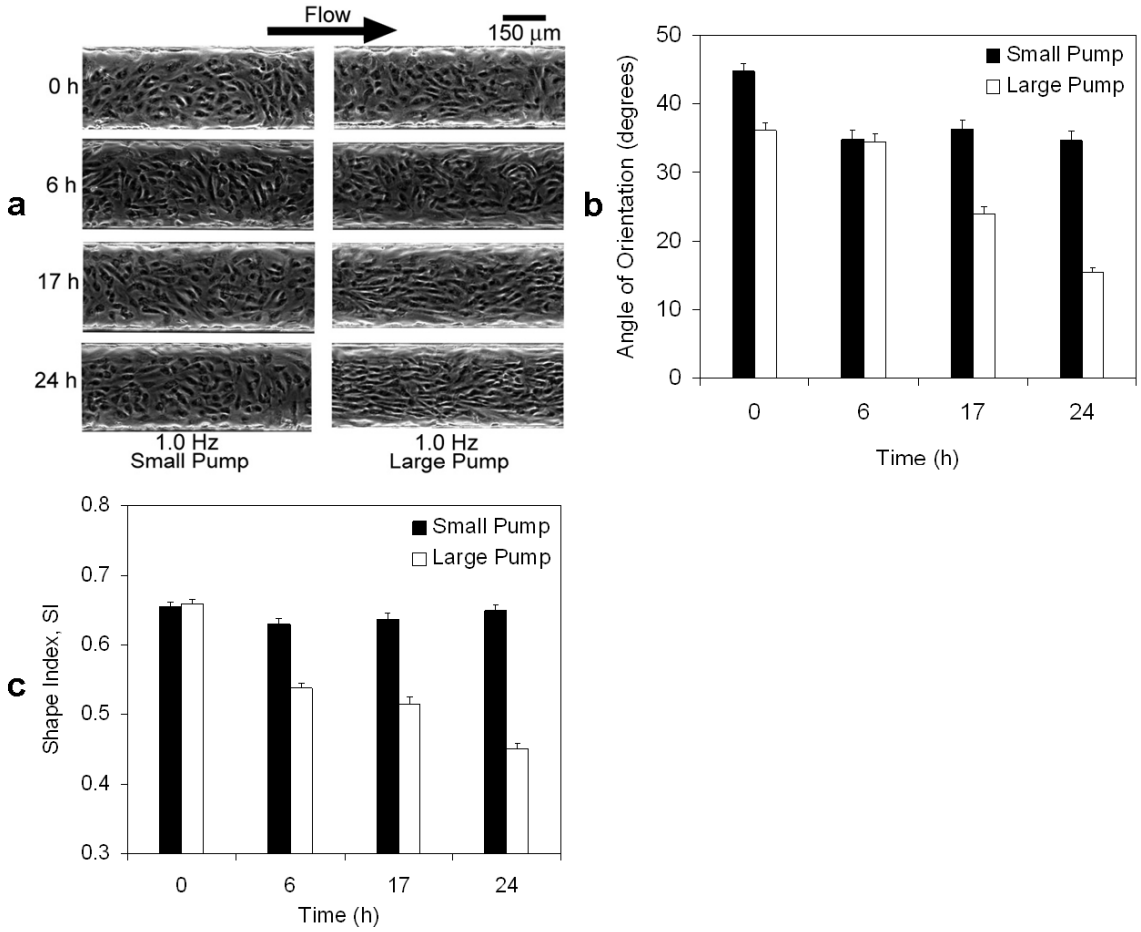

Figure II.3. Cell morphology response to cell shearing conditions. (a) Time-lapse images comparing changes in cell morphology between small and large pumps circulated at the same pumping frequency (1.0 Hz). Quantification of cell alignment (b) and elongation (c) comparing the EC response due to circulation in one loop by the small pump and the other loop by the large pump both circulated at a pumping frequency of 1.0 Hz.

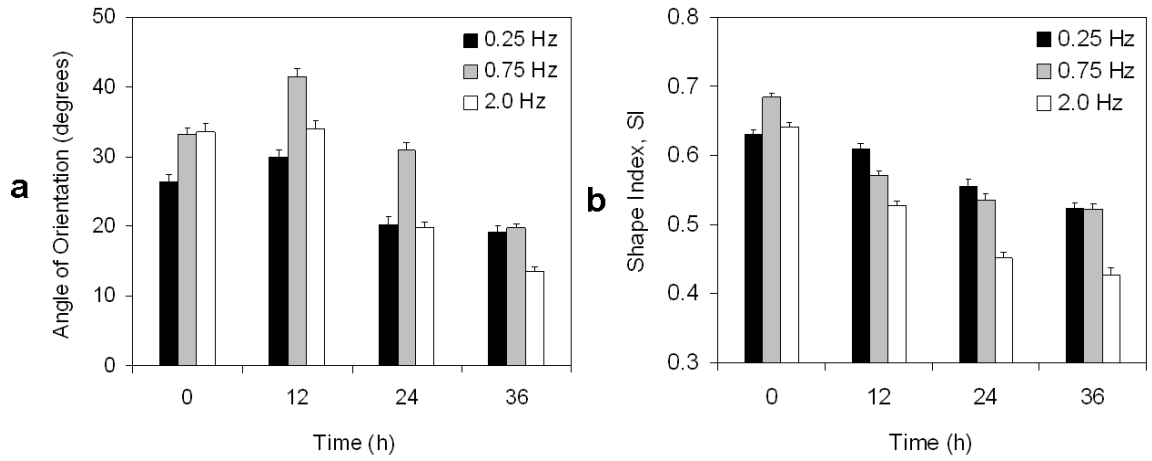

Figure II.4. Morphological response of cells subjected to different levels of cell shearing conditions. Quantification of cell alignment (a) and elongation (b) comparing EC response in three loops due to circulation by the large pump circulated at frequencies of 0.25 Hz, 0.75 Hz, and 2.0 Hz respectively.

References

1. Jeon, N. L.; Baskaran, H.; Dertinger, S. K. W.; Whitesides, G. M.; Water, L. V. D.; Toner, M. *Nat. Biotechnol.* **2002**, *20*, 826–830.

2. Takayama, S.; McDonald, J. C.; Ostuni, E.; Liang, M. N.; Kenis, P. J. A.; Ismagilov, R. F.; Whitesides, G. M. *Proc. Natl. Acad. Sci. USA*. **1999**, *96***,** 5545–5548.

3. Unger, M. A.; Chou, H.-P.; Thorsen, T.; Scherer, A.; Quake, S. R. *Science*. **2000,** *288***,** 113-116.

4. Walker, G. M.; Zeringue, H. C.; Beebe, D. J. *Lab Chip*. **2004**, *4*, 91-97.

5. Chen, C. S.; Mrksich, M.; Huang, S. Whitesides, G. M.; Ingber, D. E. *Science.* **1997,** *276*, 1425-1428.

6. Borenstein, J. T.; Terai, H.; King, K. R.; Weinberg, E. J.; Kaazempur-Mofrad, M. R.; Vacanti, J. P. *Biomed. Microdev.* **2002**, *4*, 167-175.

7. Tang, M. D.; Golden, A. P.; Tien, J. *J. Am. Chem. Soc.* **2003**, *125*, 12988-12989.

8. Bhatia, S. N.; Yarmush, M. L.; Toner, M. *J. Biomed. Mater. Res.* **1997,** *34*, 189-199.

9. Li, N.; Tourovskaia, A.; Folch, A. *Crit. Rev. Biomed. Eng.* **2003**, *31*, 423-488.

10. Gray, B. L.; Lieu, D. K.; Collins S. D.; Smith R. L.; Barakat A. I. *Biomed. Microdev*. **2002**, *4*, 9-16.

11. Fisher, A. B.; Chien, S.; Barakat, A. I.; Nerem, R. M. *Am. J. Physiol. Lung Cell Mol. Physiol.* **2001**, *281*, L529-L533.

12. Davies, P. F. *Physiol. Rev.* **1995**, *75*, 519-560.

13. Hsai, T. K.; Cho, S. K.; Honda, H. M.; Hama, S.; Navab, M.; Demer, L. L.; Ho, C. M. *Ann. Biomed. Eng.* **2002**, *30*, 646-656.

14. Helmlinger, G.; Geiger, R. V.; Schreck, S.; Nerem, R. M. *J. Biomech. Eng.* **1991**, *113*, 123-131.

15. Wojciak-Stothard, B.; Ridley, A. J. *J. Cell Biol.* **2003**, *161*, 429-439.

16. Helmlinger, G.; Berk, B. C.; Nerem, R. M. *Am. J. Physiol.* **1995**, *269*, 367-375.

17. Boo, Y. C.; Hwang, J.; Sykes, M.; Michell, B. J.; Kemp, B. E.; Lum, H.; Jo, H. *Am. J. Physiol. Heart Circ. Physiol.* **2002**, *283*, H1819-28.

18. Garcia-Cardeña, G.; Comander, J.; Anderson, K. R.; Blackman, B. R.; Gimbrone, Jr., M. A. *Proc. Natl. Acad. Sci. USA*. **2001**, *98*, 4478-4485.

19. Malek, A. M.; Gibbons, G. H.; Dzau, V. J.; Izumo, S. *J. Clin. Invest.* **1993**, *92*, 2013-2021.

20. Girard, P. R.; Nerem, R. M. *J. Cell. Physiol.* **1995**, *163*, 179-193.

21. Blackman, B. R.; García-Cardeña, G.; Gimbrone, Jr., M. A. *J. Biomech. Eng.* **2002**, *124*, 397-407.

22. Gu, W.; Zhu, X; Futai, N; Cho, B. S.; Takayama, S. *Proc. Natl. Acad. Sci. USA*. **2004**, *101*, 15861-15866.

23. Futai, N.; Gu, W.; Takayama, S. *Adv. Mater*. **2004**, *16*, 1320-1323.

24. Duffy, D. C.; McDonald, J. C.; Schueller, O. J. A.; Whitesides, G. M. *Anal. Chem.* **1998**, *70***,** 4974-4984.

25. Zhu, X.; Mills, K. L.; Peters, P. R.; Bahng, J. H.; Liu, E. H.; Shim, J.; Naruse, K.; Csete, M. E.; Thouless, M. D.; Takayama, S. *Nat. Mater.* **2005**, *4*, 403-406.

26. Loudon, C.; Tordesillas, A. *J. Theor. Biol.* **1998,** *7*, 63-78.

27. Wégria, R.; Frank, C. W.; Wang, H.; Lammerant, J. *Circ. Res.* **1958**, *6*, 624-632.

28. Levesque, M. J.; Nerem, R. M. *J. Biomech. Eng.* **1985**, *107*, 341-347.

CHAPTER III

Quantitative Real-time Imaging of Evaporation-mediated Responses of Endothelial Cells Under Sub-microliter Recirculation Culture

Compared to conventional cell cultures performed in Petri dishes with low cell volume to extracellular fluid volume (CV/EV) ratios, microfluidic environments with large CV/EV ratios have many advantages in terms of cellular self-conditioning of their surrounding medium.[1] Systems with large CV/EV ratios, however, typically also possess large surface to volume (SAV) ratios which increases the rate of evaporation and presents a challenge, particularly when using microfluidic devices made of water vapor permeable materials such as poly(dimethylsiloxane) (PDMS). Although understanding and preventing evaporation is generally important for microfluidic applications, it is particularly crucial for sensitive mammalian cell culture applications where even relatively small shifts in osmolality can drastically alter cell behavior.[2-6] Here we provide a practical solution that is demonstrated specifically for human dermal microvascular endothelial cell (HDMEC) culture in microfluidics by utilizing a PDMS-parylene-PDMS "hybrid" membrane. These membranes can prevent such evaporation to enable long-term culture (~12h) of HDMCs under continuous recirculation of sub-microliter amounts of fluid while also providing the mechanical flexibility needed to be compatible with deformation-based microfluidic actuation systems and the optical clarity needed for cell imaging. We also have expanded the capabilities of this system to include real-time imaging of cellular response in the compartment of interest by customizing the actuation

system[7] to fit on the stage of an inverted phase contrast microscope. The ability to stabilize evaporation in PDMS chips compatible with pin actuator-based computer controlled pumps and valves using the PDMS-parylene-PDMS "hybrid" membrane expands the ability to perform convenient and versatile microfluidic cell culture experiments where fluid circulation and exchange can be regulated to mimic the dynamic culture environments *in vivo* or to manipulate reagents for long-term on-chip assays.

Experimental Section

Parylene deposition. For parylene coated PDMS, 2.5 or 5μm thick layer of parylene C was deposited on the backside of PDMS membranes by using a PDS 2010 labcoater (Specialty Coating Systems) after covering the well side with a PDMS membrane.

Device Fabrication for Microfluidic Endothelial Cell Culture. The microfluidic device for endothelial cell (EC) culture was fabricated as was described previously.[8] Briefly, three layers of cured poly(dimethylsiloxane) (PDMS) at a ratio of 10:1 base to curing agent were sealed together irreversibly using plasma oxidation (SPI supplies, West Chester, PA). Unless stated otherwise, the PDMS layers were cured overnight at 60^{o}C. The top of the three layers (~1 cm thick) contains a rectangular shaped fluid reservoir (Figure 6a). The middle layer (~1 mm thick) consists of bell-shaped channels features[9] ~30 μm in height and 300 μm in width formed using soft lithography.[10] The channel features of the middle layer face downward and are sealed

against a thin membrane bottom layer which is the substrate for cell attachment. PDMS-only thin membranes were fabricated by spin coating freshly mixed 1:10 PDMS onto silanized (75 x 50 mm, 1mm thick) glass slides (Corning Glass Works, Corning, NY**)** to a uniform thickness of either ~120 and 400 μm and then cured overnight at 120^{o}C. For experiments involving parylene coated membranes, the same PDMS-parylene-PDMS hybrid thin membrane described above with a total uniform thickness of 200 μm was used.

Fluid Actuation System. The computer-controlled Braille display fluid actuation scheme is based on a design described previously[7] with minor modifications to make the system more compatible with inverted phase contrast microscopy.[11] The Braille display used (SC9; KGS, Saitama, Japan) was powered by a universal serial bus (USB) and consisted of 8 actuation cells, each containing 8 piezoelectric Braille pins (8 × 8 = 64 pins).

Indium tin oxide (ITO) Heater. The ITO heater was constructed by an ITO layer deposited on a glass slide with metallic films for electric contact. First, the glass slide was masked using scotch tape to form the pattern for the ITO layer. An ITO with a thickness of ~1500Å was coated on a 75x25x1 mm slide glass using radio frequency sputtering (Enerjet Sputter) as shown in Figure III.1. This is followed by removing the masking tapes and annealing the device in a 650^{o}C convection oven for 1 hour. The resulting sheet resistance of the annealed ITO layer is ~30 Ω/square. In order to smoothly generate electric current through the ITO layer for uniform joule heating,two

aluminum strips (1 mm width and 2000Å thick) were patterned and coated in a similar manner on two edges of the ITO layer. Electrical wires were attached to the aluminum stripes using silver epoxy glue to form connections to external control circuits. A commercially available wire thermocouple (5TC-TT-J; Newport, Santa Ana, CA) was attached onto the heater surface for temperature sensing. All the wires were connected to a microprocessor based temperature control unit (CT16A2088, Minco Products, Inc., Minneapolis, MN) for feedback control of the heater surface temperature. As a result, the heater surface can be maintained constantly at desired temperature. The advantages of this ITO heater are: 1) excellent optical transparency in visible light wavelength range, 2) less image distortion than thin film heater.[7], and 3) more uniform heating over large areas.

General Endothelial Cell Culture. Human dermal microvascular endothelial cells (HDMECs, Cambrex, East Rutherford, NJ) were cultured in endothelial growth media-2 MV (EGM-2 MV, Cambrex) in T-25 culture flasks (Corning, Acton, MA) that were placed in a humidified 5% CO_2 cell culture incubator. The HDMECs were collected by washing and detaching with 0.25% Trypsin/EDTA (Invitrogen, Carlsbad, CA). The Trypsin solution was neutralized with 10% FBS in DMEM and spun down with a centrifuge (ThermoForma, Marietta, OH) for 5 min, 4^{o} C, 800 RPM. The supernatant was removed and the pellet was resuspended in EGM-2 MV. The spin and resuspension in EGM-2 MV was repeated to ensure removal of Trypsin which inhibits cell adhesion during seeding.

Cell Seeding and Microfluidic Cell Culture. To facilitate cell attachment, the channels were coated for 30-60 min at room temperature with 5-10 μl of human plasma fibronectin (FN) solution (Invitrogen) at a concentration of 100 μg/ml PBS shortly after plasma oxidation (5-10 min). The FN solution was introduced through holes punched with a dermal biopsy puncher (Miltex Inc., York, PA) though the top and middle layer prior to sealing with plasma oxidation to act as seeding ports by being compatible for use with micropipette tips. After cell seeding (described below), the seeding ports were covered with a sterilized glass slide to avoid contamination when present in non-sterile conditions. After coating, the FN solution was rinsed for 10 minutes with PBS that was pumped through the channels from the fluid reservoir. Afterwards, the device was sterilized by placing under UV light for ~30 minutes. Following UV sterilization, PBS was replaced with endothelial growth media-2 MV (EGM-2 MV, Cambrex, East Rutherford, NJ) which is supplemented as a kit prior to use with 5% fetal bovine serum (FBS) and a host of growth factors/supplements such as vascular endothelial growth factor (VEGF). EGM-2 MV was circulated overnight for the serum proteins to coat the PDMS surface along with FN to facilitate cell attachment. All reagents were added under sterile conditions.

A small amount (3-5 μl) of a dense (~10^7 cells/ml) HDMEC suspension was pipeted into the cell seeding port and introduced into fluidic regions defined by the Braille pins acting as valves via gentle application of positive pressure. After the HDMECs were seeded, all channels were valved to trap the cells and the PDMS chip and the Braille display were placed in a 37^{o}C/5% CO_2 incubator to allow for the cells to

attach for 60-90 minutes. After the cells attach, EGM-2 MV culture media was circulated from the fluid reservoir for the next 24-72 h until the cells reach confluence.

Recirculating Fluid Actuation. Experiments conducted with recirculation of small amounts of fluid (~500 nl) were conducted on the stage of an inverted microscope (Nikon TS-100F, Japan), imaged with a 10x Ph1 objective (Achromat), and recorded using Coolsnap CF2 Camera with MetaVue software. To account for the lack of controlled temperature and 5% CO_2 tension provided by a cell culture incubator, the bottom of the PDMS device was heated to 37^{o}C (ITO heater, PID Temperature Controller, Minco, Minneapolis, MN) and the culture media was specially formulated with a synthetic buffer to maintain stable pH of ~7.3 under ambient conditions.[7]

Braille pins were reconfigured via computer-control such that flow can only occur in the recirculation loop (Figure III.2a) due to complete valving. The initial amount of fluid continuously recirculated was ~500 nl at a pumping frequency of 0.125 Hz. Images were recorded at the intersection of the "X" towards the center of the microfluidic device (Figure III.2a). The cell density was recorded for discrete time points and normalized to the value at T=0. Cells were considered still alive if they remained attached and were still moving (visualized with real-time microscopy). For PDMS-only membranes, two experiments were performed in duplicates; for the Parylene membrane device, only one experiment was performed.

Results and Discussion

Endothelial Cell Survival Under Recirculating Fluid Actuation. Using the deformation-based fluid actuation described above that incorporates a PDMS-parylene-PDMS hybrid membrane, we also tested sub-microliter recirculating culture of human dermal microvascular endothelial cells (HDMEC) in a non-humidified environment with on device heating. This type of capability is expected to be important for future studies of the effect of autocrine and paracrine effects on endothelial cells under fluid perfusion conditions.

Confluent monolayers of HDMECs were seeded and cultured within the microfluidic device and imaged at the intersection of the "X" region (Figure III.2a). Figure III.2b is a timelapse comparison of HDMEC survival under continuous recirculation of ~500 nl of media with deformation-based Braille fluid actuation. The experimental conditions were 120 μm thick, PDMS-only membrane ("thin PDMS"); 400 μm thick, PDMS-only membrane ("thick PDMS"); and 200 μm thick, PDMS-parylene hybrid membrane ("hybrid"). At T = 40 (time given in min), virtually all the cells in the visualized region for the "thin PDMS" membrane are dead and detached whereas the cells for the "thick PDMS" and "hybrid" membranes remain confluent. At T = 80, virtually all the cells for the "thin PDMS" and "thick PDMS" membranes are dead and detached whereas the "hybrid membrane" still remains confluent.

The results were quantified by counting the changes in cell density with time due to continuous recirculation (Figure III.2c). For the "thin PDMS" membrane, about 50 percent of the cells were dead and detached by about T = 25 (extrapolating from data in Figure III.2c) and all of the cells were gone by T=50. For the "thick PDMS" membrane, about 50 percent of the cells were dead and detached by T = 65 and all of the cells were gone by T = 90. With the "hybrid" membrane, cells survive much longer under continuous recirculation than the PDMS-only membranes. Cells remain roughly confluent (>85 percent of the original cell density) up to T = 720 (or 12h). Afterwards, cells begin to die more rapidly with 50 percent of the cells remaining alive and attached at about T=800 (13.3h) and less than 5 percent at T = 1080 (18h) (Figure III.2c). By comparing the times it takes for 50 percent of the cells to die, we conclude that cells are able to survive about 2.6 times longer with the "thick PDMS" membrane compared to the "thin PDMS" membrane. In addition, cells are able to survive about 29 times as long with the "hybrid" membrane when compared with the "thin PDMS" membrane and 11 times as long when compared with the "thick PDMS" membrane. Thus, the integration of parylene in the "hybrid" membrane substantially increases the time HDMECs survive under continuous recirculation of ~500 nl of fluid even though at 200 μm, the "hybrid" membrane is slightly thicker than the "thin PDMS" membrane (120 μm) and half as thick as the "thick PDMS" membrane (400 μm).

Conclusion

Compared to conventional cell cultures performed in Petri dishes with low cell volume to extracellular fluid volume (CV/EV) ratios, microfluidic environments with large CV/EV ratios have many advantages in terms of cellular self-conditioning of their surrounding medium.[1] Systems with large CV/EV ratios, however, typically also possess large surface to volume (SAV) ratios which increases the rate of evaporation and presents a challenge, particularly when using microfluidic devices made of water vapor permeable materials such as PDMS. Although understanding and preventing evaporation is important for microfluidic applications generally, it is particularly crucial for sensitive mammalian cell culture applications where even relatively small shifts in osmolality can drastically alter cell behavior. Our study provides the following conclusions: 1) under non-humidified conditions with heating, both the 120μm- and 400μm–PDMS bottom membranes limit HDMEC survival to 25-65 minutes, and 2) PDMS-parylene-PDMS "hybrid" membranes can prevent such evaporation while also providing the mechanical flexibility needed to be compatible with deformation-based microfluidic actuation systems and the optical clarity needed for cell imaging.

The better quantitative understanding of how the osmolality of cell culture media changes in PDMS devices may be useful in accounting for and remedying such shifts in culture or for application where changes in the osmolality of media in a controlled manner during culture is necessary.[12] The ability to stabilize evaporation in PDMS chips compatible with pin actuator-based computer controlled pumps and valves using the

PDMS-parylene-PDMS hybrid membrane expands the ability to perform convenient and versatile microfluidic cell culture experiments where fluid circulation and exchange can be regulated to mimic the dynamic culture environments *in vivo* or to manipulate reagents for long-term on-chip assays.

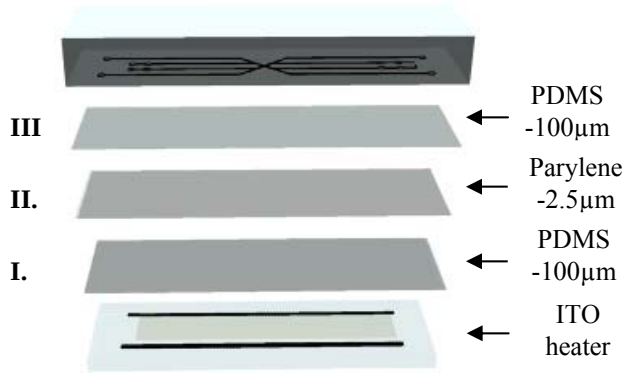

Figure III.1. Schematic representation of Braille display-based microfluidics. A typical design for Braille display-based microfluidics is composed of two layers: Upper bulk PDMS with microchannel and bottom membrane. To test the suitability of the parylene coated PDMS with Braille displays, bottom membrane consists of three layers: 100µm-PDMS, 2.5µm-parylene and 100um-PDMS. For cell culture an ITO heater, composed of a glass slide with ITO thin film (thickness about 1500Å) and aluminum electrodes (thickness about 2000Å) patterned on top of it, is placed underneath the membrane.

Figure III.2. Microfluidic device for HDMEC culture with recirculation. (a) View from the top schematic depicting the location of the Braille pins used for valving and pumping, microfluidic channels, and fluid reservoir. The fluid reservoir has a total volume of ~1 ml and completely surrounds the channel features like a picture frame to provide an unobstructed view of the cells seeded within the channels. Cut-away view shows the location of cells seeded towards the center of the device and recirculation loop with images recorded at the intersection of the "X." (b) Qualitative data showing effects of evaporation on cell viability. Timelapse images for the three experimental conditions for thin membrane: 120 micron, PDMS-only ("thin PDMS," ○), 400 micron, PDMS-only ("thick PDMS" □) and 200 micron, PDMS-parylene hybrid membrane ("hybrid" ◇). Time listed is in minutes. (c) Quantitative data describing effects of evaporation on cell viability. Cell density was normalized to values at T=0.

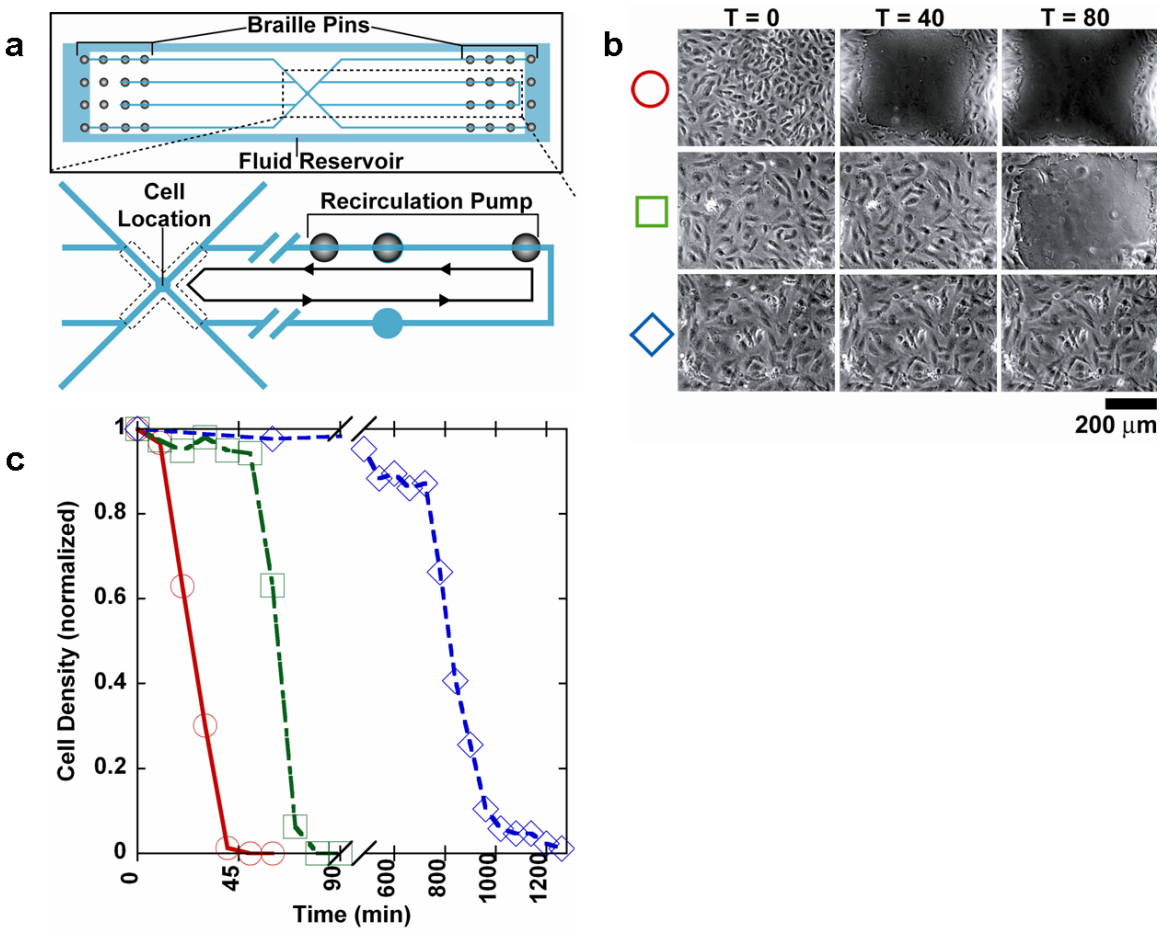
a
Braille Pins
Fluid Reservoir
Cell Location
Recirculation Pump
b
T = 0
T = 40
T = 80
200 μm
c
Cell Density (normalized)
Time (min)
0
0.2
0.4
0.6
0.8
1
0
45
90
600
800
1000
1200

References

1. Walker, G. M.; Zeringue, H. C.; Beebe, D. J., Microenvironment design considerations for cellular scale studies. *Lab Chip* **2004,** 4, (2), 91-7.

2. Hu, W. S.; Aunins, J. G., Large-scale mammalian cell culture. *Curr Opin Biotechnol* **1997,** 8, (2), 148-53.

3. Lezama, R.; Diaz-Tellez, A.; Ramos-Mandujano, G.; Oropeza, L.; Pasantes-Morales, H., Epidermal growth factor receptor is a common element in the signaling pathways activated by cell volume changes in isosmotic, hyposmotic or hyperosmotic conditions. *Neurochem Res* **2005,** 30, (12), 1589-97.

4. Moor, A. N.; Murtazina, R.; Fliegel, L., Calcium and osmotic regulation of the Na+/H+ exchanger in neonatal ventricular myocytes. *J Mol Cell Cardiol* **2000,** 32, (6), 925-36.

5. Ozturk, S. S.; Palsson, B. O., Growth, metabolic, and antibody production kinetics of hybridoma cell culture: 1. Analysis of data from controlled batch reactors. *Biotechnol Prog* **1991,** 7, (6), 471-80.

6. Wu, M. H.; Dimopoulos, G.; Mantalaris, A.; Varley, J., The effect of hyperosmotic pressure on antibody production and gene expression in the GS-NS0 cell line. *Biotechnol Appl Biochem* **2004,** 40, (Pt 1), 41-6.

7. Futai, N.; Gu, W.; Song, J. W.; Takayama, S., Handheld recirculation system and customized media for microfluidic cell culture. *Lab Chip* **2006,** 6, (1), 149-54.

8. Song, J. W.; Gu, W.; Futai, N.; Warner, K. A.; Nor, J. E.; Takayama, S., Computer-controlled microcirculatory support system for endothelial cell culture and shearing. *Anal Chem* **2005,** 77, (13), 3993-9.

9. Futai, N.; Gu, W.; Takayama, S., Rapid prototyping of microstructures with bell-shaped cross-sections and its application to deformation-based microfluidic valves. *Advanced Materials* **2004,** 16, (15), 1320-+.

10. Duffy, D. C.; McDonald, J. C.; Schueller, O. J. A.; Whitesides, G. M., Rapid prototyping of microfluidic systems in poly(dimethylsiloxane). *Analytical Chemistry* **1998,** 70, (23), 4974-4984.

11. Mehta, G.; Mehta, K.; Sud, D.; Song, J. W.; Bersano-Begey, T.; Futai, N.; Heo, Y. S.; Mycek, M. A.; Linderman, J. J.; Takayama, S., Quantitative measurement and control of oxygen levels in microfluidic poly(dimethylsiloxane) bioreactors during cell culture. *Biomed Microdevices* **2007,** 9, (2), 123-34.

12. Hay-Schmidt, A., The influence of osmolality on mouse two-cell development. *J Assist Reprod Genet* **1993,** 10, (1), 95-8.

Chapter IV

Engineered Compartmentalized Microfluidic Endothelium for Studying the Intravascular Adhesion of Metastatic Breast Cancer Cells

The ability to properly model the intravascular steps in metastasis is essential in identifying key physical, cellular, and molecular determinants that can be targeted therapeutically to prevent metastatic disease[1-4]. Research on the vascular microenvironment has been hindered by challenges in studying this compartment in metastasis under conditions that reproduce *in vivo* physiology while allowing facile experimental manipulation. Here we present a compartmentalized microfluidic vasculature system to model interactions between circulating cancer cells with vascular endothelium at potential sites of metastasis. The microfluidic vasculature is designed to produce spatially-restricted stimulation with pro-inflammatory cytokines, chemokines, or chemokine receptor inhibitors that model organ-specific localization of specific signalling molecules *in vivo* under variable flow conditions. Using this system to produce selective stimulation with CXCL12, a chemokine strongly implicated in metastasis[5-8], we established that activated endothelial cells confer site-specific adhesion of circulating cancer cells independent of CXCR4 or CXCR7 receptors on tumor cells. This combination of microfluidic technology with cancer biology provides a unique physiologic system to reproduce the intravascular microenvironment in metastasis and elucidate new cellular and molecular targets for cancer therapy.

Metastatic disease is the cause of death in approximately 90% of patients with solid tumors[9], emphasizing that preventing and/or effectively treating metastases is the primary obstacle to curing cancer. Trafficking of cancer cells through the circulation and arrest of these cells at secondary sites are obligatory steps in metastasis. Specific molecular interactions between circulating cancer cells and vascular endothelium are proposed to control organ-specific patterns of metastasis for breast[10], lung[8], and other common solid cancers[11], but our knowledge of these signals is lacking. In particular, the chemokine CXCL12 is proposed to promote tropism of malignant breast[7], lung[8], and other cancer cells for characteristic sites of metastatic disease, which has been attributed predominantly to signalling through the receptor CXCR4 on cancer cells. However, mechanisms of action for CXCL12 in metastasis also may be regulated through CXCR4 on vascular endothelium[12] and/or CXCR7[13], a newly identified second receptor for CXCL12[14].

Here, we present a systematic study using a compartmentalized microfluidic vasculature together with genetically engineered cancer cells to establish effects of CXCR4 versus CXCR7 on both the endothelium and cancer cells. The results show that with compartmentalized extravascular stimulation of the endothelium, activation of CXCR4 and possibly CXCR7 on endothelial cells can play significant roles in promoting cancer cell adhesion regardless of presence of these receptors on cancer cells. These results clarify the role of CXCL12 in the intravascular steps of metastasis and provide insights for identifying therapeutic targets to block metastasis. The results also highlight

the versatility and utility of the microfluidic vasculature system to enable studies, such as compartmentalized extravascular stimulation of select regions of an endothelium, that would be too complex, non-physiological or too expensive to perform using conventional in vivo [15, 16] or in vitro assay systems.

The microfluidic vasculature is comprised of two poly(dimethysiloxane) (PDMS) layers sandwiching a thin, porous, and optically clear polyester membrane (Fig. 1a). The top PDMS layer features a channel with a funnel–shaped inlet that intersects regionally distinct, perpendicularly-oriented channels in the bottom PDMS layer (Fig. 1b, c). The top channel (60 μm height, 800 μm width) contains a confluent monolayer of human dermal microvascular endothelial cells (HDMECs) (Fig. 1e) cultured on a thin polyester membrane with 400 nm pores that permits the transport of biomolecules but not cells between the top and bottom channels. The regions of the top channel that intersect one of the bottom channels (60 μm height) are referred to as either the upstream or downstream compartment (Figs. 1c-e), depending on the location relative to the funnel-shaped inlet. The region between the upstream and downstream compartments with no lower channel is referred to as the middle compartment. The dimensions of each compartment are 4400 μm (or 4.4 mm) long by 800 μm wide.

Endothelial cells in the upstream and downstream compartment can be region selectively treated with biomolecules from the lower channels. We observed that staining

of a confluent endothelium with Syto 64 remains well-defined within the desired compartments for at least 5.5 hours (Fig. 1d). Furthermore, we observed statistically greater adhesion of circulating MDA-MB-231[17] (or 231-control) breast cancer cells onto the endothelial compartment treated with the pro-inflammatory cytokine TNF-α compared to the untreated endothelial compartment at shear stress levels of 0.50 dyn/cm^2 and 2.50 dyn/cm^2 (Fig. 1 f-h) ($p < 0.02$). The spatial control afforded by the system enabled direct comparison of cancer cell adhesion onto stimulated versus non-stimulated regions of endothelium. We note that in our system, the shear stress levels of 0.50 dyn/cm^2 and 2.50 dyn/cm^2 correspond with flow velocities of 0.2 mm/s and 1.0 mm/s respectively. These velocities are in line with the *in vivo* blood flow velocity range of 0.1-1.5 mm/s reported in the microcirculation of potential sites of breast cancer metastasis[18-20] In addition, integrins on the surface of circulating cells are reported to optimally mediate adhesion onto endothelium at shear stress levels below 0.5 dyn/cm^2 with the avidity decreasing rapidly with higher shear stress levels[21]. .

We utilized the ability to region selectively stimulate the endothelium in our microfluidic system to recreate the local stimulation with CXCL12 of tissues that are common sites for metastatic breast cancer *in vivo*[7]. The experiments address an under-studied topic on how CXCL12 and receptors CXCR4 and CXCR7 on vascular endothelium, rather than on cancer cells, may be key determinants in the intravascular adhesion step of metastasis. CXCL12 signaling in endothelium is known to upregulate and activate adhesion molecules, promoting stable interactions with circulating cells[22]. We specifically characterized the responses of the described endothelial cells (HDMECs) to CXCL12 and TNF-α. These cells are isolated from skin, a tissue with low metastatic

potential for breast cancer[10], and facilitate low amounts of adhesion of cancer cells under unstimulated conditions[23]. Under basal culture conditions, HDMECs express low levels of CXCR4 and no CXCR7 mRNA (Fig 3a). When treated with CXCL12 (100 ng/ml, 5h) HDMECs increase expression of CXCR4 but continue to not express CXCR7. When treated with TNF-α (50 ng/ml, 5h), relative to basal conditions, endothelial cells increase expression of CXCR4 and also express CXCR7. CXCL12 initiates signaling in HDMECs as evidenced by activation of AKT (Fig. 2b), a known downstream effector of CXCR4[24] and potentially CXCR7[25].

Next, we evaluated how CXCL12 and TNF-α stimulation of HDMECs independently or cooperatively modulate adhesion of 231-control breast cancer cells onto the endothelium. We compared the following combinations: 1) CXCL12 only, 2) CXCL12+AMD3100 (a competitive inhibitor of CXCR4[26]), 3) CXCL12 + TNF-α, 4) CXCL12 + TNF-α + AMD3100, and 5) TNF-α only (Fig. 2c, d). The levels of 231-control breast cancer cell adhesion onto the five different treatment conditions were significantly different ($p < 0.05$) for both the 0.50 dyn/cm^2 and 2.50 dyn/cm^2 flow conditions (Fig. 2c, d). Conversely, the levels of cancer cell adhesion onto the five corresponding untreated endothelium were statistically the same ($p > 0.85$) for both flow conditions. With the exception of the CXCL12+AMD3100 condition, adhesion of 231-control cancer cells was significantly greater onto each of the treated compartments than onto the corresponding untreated compartments for both flow conditions (Fig.2c, d) ($p < 0.05$). Treatment of endothelium with both CXCL12 + TNF-α produced additive

increases in adhesion of circulating 231-control cells relative to CXCL12 only and TNF-α only treated endothelium under both flow conditions (Fig. 3c, d). These results suggest that each cytokine enhances cancer cell adhesion through independent mechanisms.

To determine to what extent effects of CXCL12 on endothelium are mediated through CXCR4, we used AMD3100, a specific inhibitor of CXCL12 binding to CXCR4 but not CXCR7. When added to the downstream compartment, AMD3100 completely blocked CXCL12-dependent increases in cancer cell adhesion to stimulated endothelium under 0.50 and 2.50 dyn/cm^2 flow conditions (Fig. 2c, d) ($p < 0.05$). Adding AMD3100 to CXCL12 and TNF-α also decreased adhesion of 231-control cells by a comparable percentage as the combination of AMD3100 and CXCL12 alone (Fig. 2c, d), suggesting that AMD3100 was selectively blocking adhesion mediated solely through CXCL12 but not TNF-α ($p < 0.05$). Collectively, these data with the specific chemical probe AMD3100, combined with absence of CXCR4 in 231-control cells (Fig. 3a), indicate that CXCL12 signals through endothelial CXCR4 to promote adhesion of circulating breast cancer cells.

Previous reports have shown that CXCR4 expression in cancer cells promotes metastasis to distant organs such as the lung[7, 27] and that CXCR7 expression in cancer cells enhances adhesion onto endothelium under static conditions[14]. We compared the 231-control cells to other MDA-MB-231 cells stably co-expressing GFP with either

CXCR4 (231-CXCR4) or CXCR7 (231-CXCR7) (Fig. 3a) to assess the role of these CXCL12 chemokine receptors on cancer cells in mediating adhesion onto endothelium under flow. The level of adhesion of all three cancer cell-types onto CXCL12 treated endothelium was significantly greater than onto the corresponding untreated endothelium under 0.50 dyn/cm^2 flow conditions ($p < 0.05$) (Fig. 3b). Comparing the three different cancer cell lines, adhesion of 231-CXCR4, 231-CXCR7, and 231-control cells was statistically different onto both the CXCL12 treated and the untreated endothelium ($p < 0.01$). Comparing pairwise, adhesion of the 231-CXCR4 and 231-CXCR7 cells was statistically greater than the 231-control cells on both the CXCL12 and untreated endothelium ($p < 0.05$). However, median ratios of cells adhering onto the CXCL12 treated endothelium relative to untreated endothelium were 1.9, 1.9, and 2.1 for the 231-CXCR4, 231-CXCR7, and 231-control cells, respectively (Fig. 3c). These ratios are statistically the same among the cell lines ($p = 0.83$). Therefore, although CXCR4 or CXCR7 expression in breast cancer cells facilitates adhesion onto endothelium, the enhancement of adhesion due to CXCL12 stimulation of the endothelium was comparable for all three cancer cell-types and independent of expression of CXCR4 or CXCR7 on cancer cells.

Herein we have described a microfluidic system that models, in a compact format, serial interactions of circulating cancer cells with vascular endothelium at metastatic and non-metastatic sites. The system represents advancement over previously described *in vitro* assay systems in that it possesses a unique blend of: 1) prolonged, basally

originating CXCL12 stimulation of vascular endothelium that models both the high levels and directionality of this chemokine characteristic of target organs for metastatic breast and many other cancers[7]; 2) compartment specific stimulation enabling direct comparison of cancer cells adhesion onto endothelium of differing metastatic potential within the same experiment; and 3) physiologically-relevant flow conditions in micron-scale channels.

Using this system, we demonstrate that CXCL12 stimulation of HDMECs enhances adhesion of circulating breast cancer cells, regardless of expression of chemokine receptors CXCR4 or CXCR7 on the cancer cells. These results indicate that responses of vascular endothelium to the surrounding molecular environment contribute substantially to intravascular adhesion of cancer cells, a phenomenon difficult to address with *in vivo*-studies. We also show that CXCR4 or CXCR7 on breast cancer cells promotes intravascular adhesion throughout the channel, supporting a mechanism through which these receptors promote metastasis under physiological flow conditions[14, 27]. Furthermore, AMD3100, a specific inhibitor of CXCR4 signaling[26], when applied to the endothelium can significantly reduce adhesion of cancer cells not expressing CXCR4 (Fig. 2c, d). Taken together, these data suggest that inhibiting chemokine receptors on endothelial cells may be of equal or greater importance for preventing initial steps of intravascular cancer cell adhesion as compared with targeting these receptors on cancer cells.

While we have focused on circulating cancer cells, this microfluidic system is a versatile platform for studying other intravascular processes, such as trafficking and adhesion of immune cells under physiological or pathological conditions. In addition, since the described system is rooted in microfabrication technology, we have established a system that can be parallelized for high-throughput experiments. By combining the convenience and cost-effectiveness of *in vitro* cell culture with key physical, cellular, and molecular components of the *in vivo* vasculature, we expect this new technology will accelerate studies of the intravascular microenvironment in metastatic cancer and development of new therapies to block this key step in metastasis.

Methods

Device fabrication. The microfluidic device (Fig. IV.1a) consisted of two channel layers of 12:1 base to curing agent poly(dimethylsiloxane) (PDMS, Sylgard 184, Dow Corning) that sandwiched a semi-porous, optically clear polyester membrane[28]. The layers were sealed together using a very thin (~10 μm) and uniform PDMS/toluene glue that provided robust, leakage-free sealing[29]. The top and bottom PDMS layers were molded as previously described[28] except the top layer featured a funnel –shaped inlet that was molded to intersect the inlet of the top channel (Fig. IV.1a). After the device was assembled, tubing was attached to the outlet of the top channel and to the inlets of the bottom channels using epoxy. Subsequently, the devices were treated with plasma oxygen (SPI Supplies, West Chester, PA) for 10 min to reduce hydrophobicity of surfaces. Immediately afterwards, the top channel was coated with a fibronectin solution

(10 μg/ml PBS, 3h, 37^{o}C). Prior to cell seeding, the device was sterilized by placing under UV light for ~ 30 min.

Endothelial cell culture and seeding. Human dermal microvascular cells (HDMECs, Lonza) passage numbers 6-8 were cultured in EBM-2 + 5% FBS + SingleQuot® kit (supplements such as VEGF, bFGF, etc) or EGM-2 MV (Lonza). A concentrated solution of HDMECs (~10^7 cells/ml EGM-2 MV) were loaded into the funnel-shaped, allowed to attach along the entire length of the top channel, and grown to confluence (24-48 h after seeding).

CXCR7 and CXCR4 expression in MDA-MB-231 human breast cancer cells. Human MDA-MB-231 breast cancer cells (ATCC) were cultured in DMEM + 10% FBS + 1% L-glutamine + 0.5% penicillin/streptomycin. Lentiviral vectors for CXCR4-GFP, CXCR7, or GFP control (Fig.3) were used to stably transduce MDA-MB-231 cells to create the described 231-CXCR4, 231-CXCR7, or 231-control cells respectively. Chemokine receptor expression in the 231-CXCR4, 231-CXCR7 cells, and 231-control cells were verified by flow cytometry (Fig. IV.3a).

RT-PCR. Endothelial cells were cultured in EBM-2 + Single®Quots with TNF-α (50 ng/ml), CXCL12 (100 ng/ml), or vehicle control for 5 hours. Total RNA was prepared using Trizol reagent (Invitrogen) according to the manufacturer's protocol. RNA was

purified further over an RNA extraction column (Qiagen), including on-column treatment with DNaseI. RT-PCR was performed using a two-step kit (ThermoScript, Invitrogen). Sequences of PCR primers were the following:

CXCR4: 5'-ACGGACAAGTACAGGCTGCAC-3' and 5'-CCCAGAAGGGAAGCGTGA-3'

CXCR7:5'-AAGAAGATGGTACGCCGTGTCGTCTC-3' and 5'-CTGCTGTGCTTCTCCTGGTCACTGGA-3'

GAPDH: 5'-GAAGGTGAAGGTCGGAGT-3' and 5'-GAAGATGGTGATGGGATTTC-3'

Western Blot. 231 breast cancer cells were cultured overnight in DMEM medium containing 0.5% serum. Breast cancer cells then were treated with 100 ng/ml CXCL12 (R&D Systems) for 3 or 10 minutes, respectively. Human dermal microvascular endothelial cells were cultured in EBM-2 + Single®Quots and treated with 100 ng/ml CXCL12 for 10 minutes or 5 hours, respectively. Total cell lysates were harvested and prepared for Western blotting as described previously[30]. Primary antibodies to AKT phosphorylated at serine 473 and total AKT (Cell Signaling) were used at 1:500 dilution, and a secondary anti-rabbit antibody conjugated with horseradish peroxidase was used at 1:2000 dilution. Western blots were developed with ECL reagent (Amersham).

Calculation of shear stress levels. The shear stress levels on the cells within the channels were modeled with the following equation[31, 32]:

$$\tau = \frac{6 \times 2.95 \mu Q_{2-D}}{h^2} \qquad (1)$$

Where τ is the shear stress on the cells, μ is the viscosity of the fluid (water = 0.01 dyn/cm^2), $Q_{2\text{-}D}$ is the flow rate per width in the system and h is the height of the channel. This equation is valid for cases where the width is much larger than the height. In our system, the height of the channels was 60 μm and the width was 800 μm.

Flow-based intravascular adhesion experiments. Prior to each experiment, the EGM-2 MV culture in the funnel-inlet of the microfludic device was removed, washed with PBS, and replaced with EBM-2 + Single®Quots. Subsequently, the top channel was washed with EBM-2 + Single®Quots by gravity flow. Concurrently, the bottom channels were triple washed with PBS and replaced with either EBM-2 + Single®Quots (untreated) or EBM-2 +Single®Quots + cytokine or chemokine of interest (treated). The flow in the top channel was stopped and the device was left to be treated for 5 h. Concurrently, culture flasks of the 231 breast cancer cells were washed with PBS and serum starved in EBM-2 + 0.5% FBS for 5 h as well. After serum starvation, the breast cancer cells were collected using citric saline, a calcium ion chelator, instead of trypsin to ensure cell surface proteins remain intact. The cancer cells were centrifuged twice and resuspended in EBM-2 + 0.5% FBS at a concentration of 2 x 10^6 cells/ml). The cancer cell suspension

was loaded into the funnel-shaped inlet. Flow was controlled using a programmable syringe pump that withdraws fluid away from the funnel-shaped inlet at flow rates corresponding with either 0.50 dyn/cm^2 or 2.50 dyn/cm^2. The microfluidic device was placed on the stage of an epi-fluorescence, inverted microscope (Nikon, TE-300). The duration of each experiment was 30 min with images were recorded every 3 min and movies 1 min in duration recorded every 10 min. For the 0.50 dyn/cm^2 experiments, the top channel was washed for 1 min at shear stress levels of 8 dyn/cm^2. To determine cell counts, fluorescent cells in the entire compartment were counted blindly and treated as one data point.

Statistical analysis. Sample populations were compared either pairwise using the Mann-Whitney U test or in groups of more than two using the Kruskal-Wallis test. These tests are nonparametric and do not require an underlying normal distribution. $p < 0.05$ was the threshold for statistical significance.

Figure IV.1: Microfluidic vasculature device enabling compartment specific activation of endothelium.

(a) Schematic of the poly(dimethysiloxane) (PDMS) microfluidic device demonstrating multi-layer fabrication with a thin, porous polyester membrane sandwiched by the top and bottom PDMS layers.
(b) Photograph of the microfluidic device loaded with different colored dye to distinguish between the top channel and the two bottom channels.
(c) Top view of the microfluidic device. During flow-based experiments, fluid is withdrawn away from the funnel-shaped inlet and through the top channel with a programmable syringe pump (see Methods).
(d) Validation of region-specific stimulation of endothelium. The upstream and downstream lower channels were filled with 25 μM Syto 64, a fluorescent dye that stains cells. HDMECs overlying the upstream and downstream bottom channels, but not HDMECs in the middle of the channel fluoresce. Fluorescence was evident within 15 minutes, remained spatially-restricted for at least 5.5 hours, and persisted after 30 minutes of flow through the top channel. Image shows 5.5 hours after initial treatment. Scale bar represents 800 μm.
(e) Phase contrast image of HDMECs cultured in the microfluidic device. The image depicts the entire length of the endothelium with the upstream, middle, and downstream compartments clearly demarcated from each other. Scale bar represents 800 μm.
(f) Representative fluorescent images of adhesion of 231-control cells (stably expressing GFP) onto region-specific TNF-α treated endothelium under 0.50 dyn/cm^2 shear stress flow conditions. In these images, the downstream compartment was treated with TNF-α (50 ng/ml for 5h) and denoted in the image with a '+' while the upstream and middle compartments were left untreated. Scale bar represents 200 μm.
(g) Quantitative analysis of 231-control cell adhesion under 0.50 dyn/cm^2 shear stress flow conditions. The inflammatory cytokine TNF-α was applied to either the upstream or downstream compartment (denoted by a '+') while the other compartment in the same device was left untreated. Significantly greater numbers of cells adhered to the TNF-α treated compartment versus the untreated compartment ($p < 0.01$) ($n = 3$ each for upstream or downstream treated conditions).
(h) Quantitative analysis of 231-control cell adhesion under 2.50 dyn/cm^2 shear stress flow conditions. TNF-α was applied to either the upstream or downstream compartment (denoted by a '+') with the other compartments in the same device left untreated. Cancer cell adhesion in the TNF-α treated compartment was significantly greater than the untreated compartment ($p < 0.01$) ($n = 3$ each for upstream or downstream treated conditions. Data are expressed as the mean + SEM.

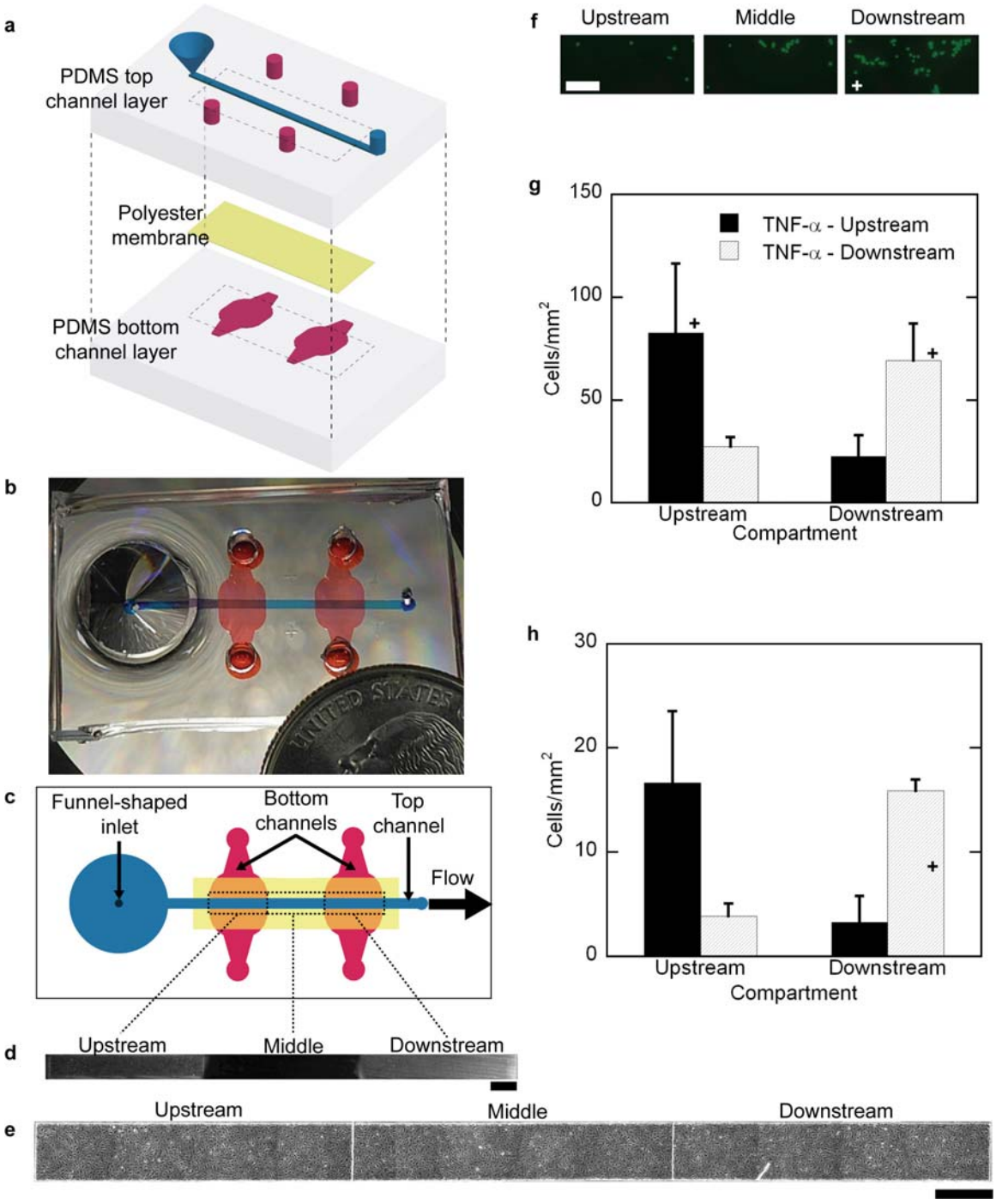
a
PDMS top channel layer
Polyester membrane
PDMS bottom channel layer
b
c
Funnel-shaped inlet
Bottom channels
Top channel
Flow
d
Upstream
Middle
Downstream
e
Upstream
Middle
Downstream
f
Upstream
Middle
Downstream
g
150
100
50
0
Cells/mm2
TNF-α - Upstream
TNF-α - Downstream
Upstream
Downstream
Compartment
h
30
20
10
0
Cells/mm2
Upstream
Downstream
Compartment

Figure IV.2: Region selective treatment of the microfluidic endothelium with combinations of cytokines and inhibitors under two different flow conditions.

(a) Chemokine receptor expression in HDMECs determined by reverse transcription PCR (RT-PCR). HDMECs show expression of CXCR4 but not CXCR7 under basal conditions. CXCL12 upregulates CXCR4 but not CXCR7. TNF-α upregulates CXCR4 and results in expression of CXCR7. RT-PCR for the housekeeping gene GAPDH confirms equivalent loading and intact RNA for all samples.

(b) CXCL12 activates AKT in endothelium. HDMECs were incubated with 100 ng/ml CXCL12 for 10 minutes or 5 hours. Control cells were incubated with BSA alone. Cell lysates were probed for phosphorylation of serine 473, and then blots were stripped and re-probed for total AKT. There is CXCL12-dependent activation of AKT that remains greater than control endothelium through 5 hours.

(c) 231-control cancer cell adhesion onto endothelium treated with different combinations of CXCL12 (100 ng/ml), TNF-α (50 ng/ml), and the CXCR4 inhibitor AMD3100 (80 ng/ml) for 5 hours under 0.50 dyn/cm^2 flow conditions. Each of the treated compartments (left four columns) was matched by color and with its corresponding untreated compartment (right four columns). Cell adhesion onto each treated compartment was compared to its corresponding untreated compartment (*, $p < 0.05$). Comparing the five treated compartments, the levels of adhesion were statistically different (**, $p < 0.05$). Conversely, for the untreated compartments, the levels of adhesion were statistically the same (#, $p = 0.85$). AMD3100 in the presence of CXCL12 decreased adhesion by 34% relative to the CXCL12 only condition. AMD3100 in the presence of CXCL12 and TNF-α decreased adhesion 42% relative to CXCL12 + TNF-α. ***, $p < 0.05$. n = 4-6 for each condition.

(d) Same as (c) except under 2.50 dyn/cm^2 flow conditions. (*, $p < 0.05$; **, $p < 0.01$; #, $p = 0.97$; ***, $p < 0.05$). Data are expressed as mean +SEM. n = 4-6 for each condition.

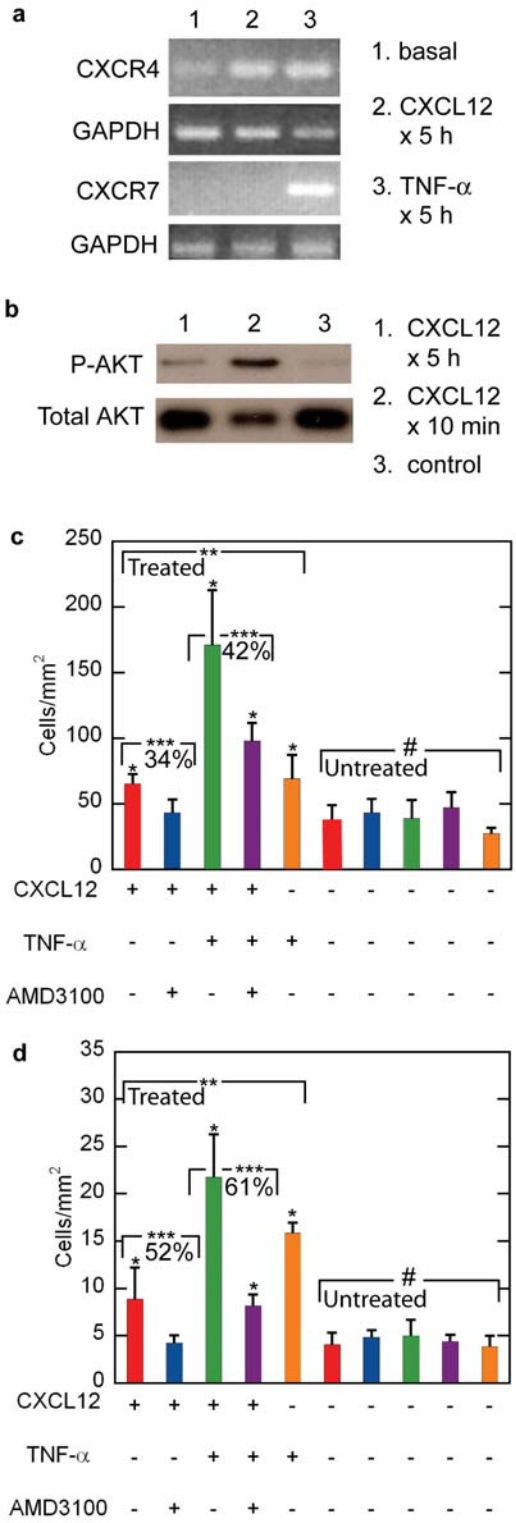
a
1 2 3
CXCR4
GAPDH
CXCR7
GAPDH
1. basal
2. CXCL12 x 5 h
3. TNF-α x 5 h
b
1 2 3
P-AKT
Total AKT
1. CXCL12 x 5 h
2. CXCL12 x 10 min
3. control
c
Cells/mm2
Treated
Untreated
34%
42%
CXCL12
TNF-α
AMD3100
d
Cells/mm2
Treated
Untreated
52%
61%
CXCL12
TNF-α
AMD3100

Figure IV.3: CXCL12 stimulated endothelium enhances adhesion of breast cancer cells.

(a) Flow cytometry with antibodies to CXCR4 (12G5) or CXCR7 (11G8) shows expression in appropriate cell lines and absence of these receptors in pSico control cells. Open symbol, isotype antibody control; filled yellow, antibody stain.
(b) CXCL12-dependent activation of AKT in 231-CXCR4 cells. Breast cancer cell lines were cultured overnight in medium containing 0.5% serum and then treated with 100 ng/ml CXCL12. Cell lysates were probed for phosphorylation of AKT at serine 473. Blots then were stripped and probed for total AKT as a loading control
(c) Compartmentalized adhesion of 231-CXCR4, 231-CXCR7, and 231-control cancer cells onto CXCL12 treated versus untreated endothelium under 0.50 dyn/cm^2 shear flow conditions. For all three cancer cell-types, the level of adhesion onto the CXCL12 treated endothelial compartment was significantly greater than onto the corresponding untreated compartment (*, $p < 0.05$). The level of adhesion of the three different cancer cell-types was statistically different on both the CXCL12 treated and untreated endothelial compartments (**, $p < 0.01$). Data are expressed as mean + SEM. $n = 6$ for all three cell-types.
(d) Boxplot representing the ratio of the levels of adhesion of cancer cells onto the CXCL12 treated endothelial compartment over the untreated compartment. Adhesion to CXCL12-stimulated endothelium was enhanced to a comparable extent for all cell lines, independent of expression of CXCR4 or CXCR7. #, $p = 0.83$.

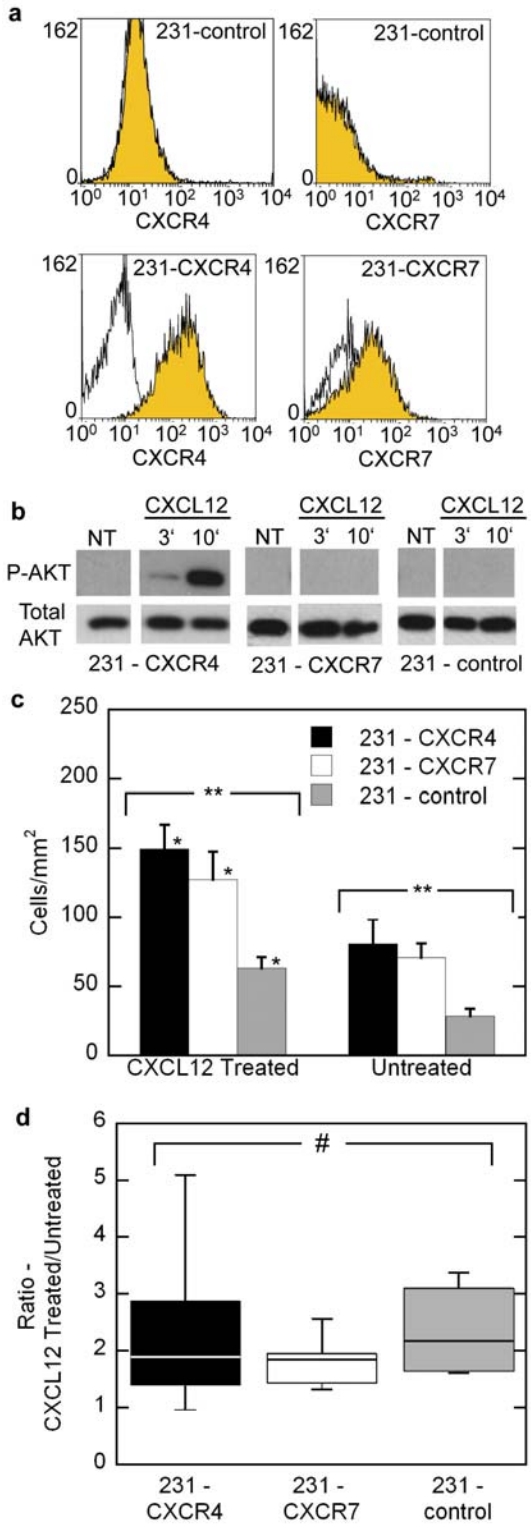
a
231-control
CXCR4
CXCR7
231-CXCR4
231-CXCR7
b
CXCL12
NT
3'
10'
P-AKT
Total AKT
231 - CXCR4
231 - CXCR7
231 - control
c
231 - CXCR4
231 - CXCR7
231 - control
Cells/mm2
CXCL12 Treated
Untreated
d
Ratio - CXCL12 Treated/Untreated
231 - CXCR4
231 - CXCR7
231 - control

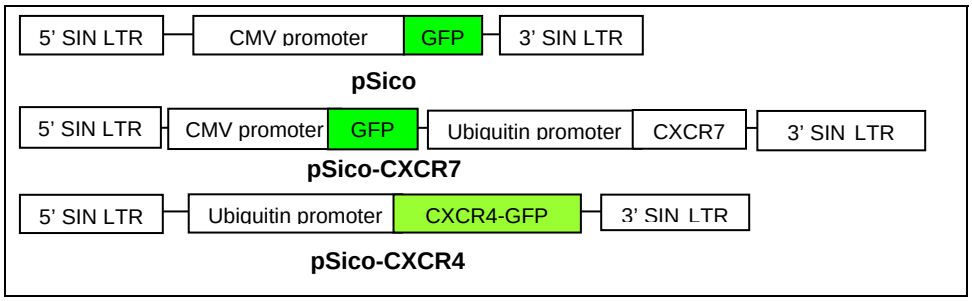

Figure IV.4: MDA-MB-231 human breast cancer cells transduced with CXCR4 or CXCR7. Schematic diagram of lentiviral constructs. CMV, cytomegalovirus immediate early promoter; SIN LTR, self inactivating long terminal repeat domain of lentiviral vector.

References

1. 1. Bockhorn, M., Jain, R.K. & Munn, L.L. Active versus passive mechanisms in metastasis: do cancer cells crawl into vessels, or are they pushed? *Lancet Oncology* **8**, 444-448 (2007).

2. Murphy, P.M. Chemokines and the molecular basis of cancer metastasis. *New England Journal of Medicine* **345**, 833-835 (2001).

3. Sahai, E. Illuminating the metastatic process. *Nature Reviews Cancer* **7**, 737-749 (2007).

4. Woodhouse, E.C., Chuaqui, R.F. & Liotta, L.A. General mechanisms of metastasis. *Cancer* **80**, 1529-1537 (1997).

5. Ali, S. & Lazennec, G. Chemokines: novel targets for breast cancer metastasis. *Cancer and Metastasis Reviews* **26**, 401-420 (2007).

6. Luker, K.E. & Luker, G.D. Functions of CXCL12 and CXCR4 in breast cancer. *Cancer Letters* **238**, 30-41 (2006).

7. Muller, A. et al. Involvement of chemokine receptors in breast cancer metastasis. *Nature* **410**, 50-56 (2001).

8. Phillips, R.J. et al. The stromal derived factor-1/CXCL12-CXC chemokine receptor 4 biological axis in non-small cell lung cancer metastases. *American journal of respiratory and critical care medicine* **167**, 1676-1686 (2003).

9. Nguyen, D.X. & Massague, J. Genetic determinants of cancer metastasis. *Nature Reviews Genetics* **8**, 341-352 (2007).

10. Weigelt, B., Peterse, J.L. & van't Veer, L.J. Breast cancer metastasis: Markers and models. *Nature Reviews Cancer* **5**, 591-602 (2005).

11. Fidler, I.J. Critical determinants of metastasis. *Seminars in Cancer Biology* **12**, 89-96 (2002).

12. Gupta, S.K., Lysko, P.G., Pillarisetti, K., Ohlstein, E. & Stadel, J.M. Chemokine receptors in human endothelial cells - Functional expression of CXCR4 and its transcriptional regulation by inflammatory cytokines. *Journal of Biological Chemistry* **273**, 4282-4287 (1998).

13. Mazzinghi, B. et al. Essential but differential role for CXCR4 and CXCR7 in the therapeutic homing of human renal progenitor cells. *The Journal of experimental medicine* **205**, 479-490 (2008).

14. Burns, J.M. et al. A novel chemokine receptor for SDF-1 and I-TAC involved in cell survival, cell adhesion, and tumor development. *Journal of Experimental Medicine* **203**, 2201-2213 (2006).

15. Feng, D., Nagy, J.A., Dvorak, H.F. & Dvorak, A.M. Ultrastructural studies define soluble macromolecular, particulate, and cellular transendothelial cell pathways in venules, lymphatic vessels, and tumor-associated microvessels in man and animals. *Microscopy Research and Technique* **57**, 289-326 (2002).

16. McDonald, D.M. & Choyke, P.L. Imaging of angiogenesis: from microscope to clinic. *Nature Medicine* **9**, 713-725 (2003).

17. Cailleau, R., Olive, M. & Cruciger, Q.V. Long-term human breast carcinoma cell lines of metastatic origin: preliminary characterization. *In vitro* **14**, 911-915 (1978).

18. Chaigneau, E., Oheim, M., Audinat, E. & Charpak, S. Two-photon imaging of capillary blood flow in olfactory bulb glomeruli. *Proc Natl Acad Sci U S A* **100**, 13081-13086 (2003).

19. Desjardins, C. & Duling, B.R. Heparinase treatment suggests a role for the endothelial cell glycocalyx in regulation of capillary hematocrit. *The American journal of physiology* **258**, H647-654 (1990).

20. Jorneskog, G., Brismar, K. & Fagrell, B. Skin capillary circulation severely impaired in toes of patients with IDDM, with and without late diabetic complications. *Diabetologia* **38**, 474-480 (1995).

21. Konstantopoulos, K., Kukreti, S. & McIntire, L.V. Biomechanics of cell interactions in shear fields. *Advanced Drug Delivery Reviews* **33**, 141-164 (1998).

22. Kryczek, I. et al. CXCL12 and vascular endothelial growth factor synergistically induce neoanglogenesis in human ovarian cancers. *Cancer Research* **65**, 465-472 (2005).

23. Murakami, T. et al. Expression of CXC chemokine receptor-4 enhances the pulmonary metastatic potential of murine B16 melanoma cells. *Cancer Res* **62**, 7328-7334 (2002).

24. Kanda, S., Mochizuki, Y. & Kanetake, H. Stromal cell-derived factor-1alpha induces tube-like structure formation of endothelial cells through phosphoinositide 3-kinase. *The Journal of biological chemistry* **278**, 257-262 (2003).

25. Wang, J. et al. The role of CXCR7/RDC1 as a chemokine receptor for CXCL12/SDF-1 in prostate cancer. *The Journal of biological chemistry* **283**, 4283-4294 (2008).

26. Hatse, S., Princen, K., Bridger, G., De Clercq, E. & Schols, D. Chemokine receptor inhibition by AMD3100 is strictly confined to CXCR4. *Febs Letters* **527**, 255-262 (2002).

27. Cardones, A.R., Murakami, T. & Hwang, S.T. CXCR4 enhances adhesion of B16 tumor cells to endothelial cells in vitro and in vivo via beta(1) integrin. *Cancer Research* **63**, 6751-6757 (2003).

28. Huh, D. et al. Acoustically detectable cellular-level lung injury induced by fluid mechanical stresses in microfluidic airway systems. *Proc Natl Acad Sci U S A* **104**, 18886-18891 (2007).

29. Chueh, B.H. et al. Leakage-free bonding of porous membranes into layered microfluidic array systems. *Analytical Chemistry* **79**, 3504-3508 (2007).

30. Luker, K.E., Pica, C.M., Schreiber, R.D. & Piwnica-Worms, D. Overexpression of IRF9 Confers Resistance to Antimicrotubule Agents in Breast Cancer Cells. *Cancer Res* **61**, 6540-6547 (2001).

31. Farokhzad, O.C. et al. Microfluidic System for Studying the Interaction of Nanoparticles and Microparticles with Cells. *Anal. Chem.* **77**, 5453-5459 (2005).

32. Gaver, D.P., III & Kute, S.M. A Theoretical Model Study of the Influence of Fluid Stresses on a Cell Adhering to a Microchannel Wall. *Biophys. J.* **75**, 721-733 (1998).

CHAPTER V

Conclusion and Future Work

Development of *in vitro*-based systems that properly model the mechanical and chemical environments of endothelial cells is necessary for advancing the understanding of vascular biology and medicine. This dissertation research contributed to the field of vascular biology by utilizing a microfluidic and microfabrication approach in improving upon the current state of the art of conventional *in vitro*-based systems. Microfluidic systems provide the capabilities to properly mimic the mechanical and chemical environments of endothelial cells at the proper length scales.[1] Herein we provide a framework for highly integrated microfluidic devices which show promise for basic biomedical research.[2] Finally, since the described systems are rooted in microfabrication technology, we have established systems that not only create more *in vivo*-like environments but can also be further parallelized for high-throughput experiments.

In Chapter II we describe a computer-controlled micro-pumping and valving system for endothelial cell culture and shearing under pulsatile flow.[3] By varying both the pumping frequency and the volume displacement per pumping stroke, we can deliver a broad range of shear stress levels to confluent monolayers of endothelial. This range of shear stress includes levels seen in the arterial vasculature[4] (~ 10 dyn/cm^2) which we show align and elongate endothelial cells. The novel aspects of this design include: 1)

multiple separate endothelial cell compartments enabling multiple cell shearing experiments in parallel and 2) a self-contained system (i.e. no external pumping system and reservoirs) which limits consumption of reagents and potential for contamination. The system described in Chapter II marks a significant step in creating a microfluidic-based platform capable of providing greater insights into the mechanisms involved with mechanotransduction of endothelial cells.

In Chapter III, we provided a practical solution to the problems with evaporation that are commonly seen in PDMS microfluidic systems. Continuous culture of cells under sub-microliter amounts of fluid is highly desired in microfluidic systems but is virtually impossible in PDMS microfluidic systems because of the material's high gas permeability.[5] We constructed a PDMS-parylene-PDMS "hybrid" membrane that dramatically reduced evaporation-mediated shifts in osmolality that are very detrimental to cell viability. By integrating the "hybrid" membrane, we were able to utilize our microfluidic pumping and valving system introduced in Chapter II to continuously culture endothelial cells while recirculating approximately 1 nl of fluid per cell for ~12 h. Furthermore, we properly buffered the culture media and adapted the pumping and valving system onto a customized stage for an inverted microscope to observe changes in endothelial cells in real-time. Consequently, we created and observed nutrient-limited conditions with recirculation that mimic conditions such as ischemia due to stroke[6] which is not readily achieved with macroscopic model systems. Combined with the described dynamic pumping and valving system, we establish a microfluidic system that could be

used to dynamically switch from recirculation culture to perfusion culture with fresh media to accurately mimic ischemia-reperfusion injury following stroke.

The results described in Chapter IV were obtained by utilizing a compartmentalized microfluidic endothelium that allowed for region-specific stimulation. We modelled the intravascular adhesion of cancer cells that initiates metastasis at secondary sites.[7] Research on the vascular microenvironment has been hindered by challenges in studying this compartment in metastasis under conditions that reproduce *in vivo* physiology while allowing facile experimental manipulation. Using the microfluidic vasculature system, we produced selective stimulation with CXCL12, a chemokine strongly implicated in metastasis[8-11] and established that activated endothelial cells confer site-specific adhesion of circulating cancer cells independent of CXCR4 or CXCR7 receptors on tumor cells. This unique combination of microfluidic technology with cancer biology provides a unique physiologic system to reproduce the intravascular microenvironment in metastasis and elucidate new cellular and molecular targets for cancer therapy.

One of the dominant driving forces behind the development of mammalian cell-based microfluidic (or "animal-on-a-chip") systems is to bridge the gap that currently exists between conventional static cell culture assays and animal studies. Animal-on-a-chip systems possess physiologically relevant complexity (e.g. flow) not present in conventional cell culture systems yet are far simpler to use than animal models.[12] As a result, it is believed that the effectiveness and toxicity of a drug compound will be easier

to spot with animal-on-chip systems than with conventional model systems.[13] Because of these attributes, animal-on-a-chip systems are of wide interest from both biologists and pharmaceutical companies. The work presented in this dissertation in recreating the vasculature in microfluidic systems and can be seen as steps towards the development of "blood vessels-on-a-chip" for studying both the biology and the response of drugs involved with vascular diseases.

The described work represents an advancement of *in vitro*-based systems for evaluating the response of endothelial cells to shear stress and the role of the vasculature in breast cancer metastasis. Despite these advances, the described systems possess certain limitations that may be addressed with future research. In Chapter II, the time-averaged shear stress levels generated in the described microfluidic system was 0-10 dyn/cm^2. In the arterial vasculature, the time-averaged shear stress levels ranges from 5-20 dyn/cm^2.[14] Thus, the system described in Chapter II is capable of the lower end of shear stress levels that is considered physiologically relevant but not the higher end. To achieve time-averaged shear stress levels greater than 10 dyn/cm^2, multiple large displacement pumps in parallel can be used to actuate fluid through a single channel. Furthermore, activating multiple pumps for a single channel would provide more versatility in the types of pulsatile flow profiles that could be generated and characterized to model the different flow profiles present in the vasculature of different parts of the body.[4]

The system described in Chapter III is capable of recirculation culture of endothelial cells by utilizing a novel and dynamic Braille-based pumping and valving scheme. However, to fully model the conditions present in ischemia following stroke, it is necessary to combine recirculation culture with acute hypoxic conditions.[6] It is challenging to achieve physiologically meaningful hypoxia in PDMS-based microfluidic systems in large part due to PDMS's high permeability and solubility to oxygen.[15] To address the current limitations of the system described in Chapter III in achieving hypoxia, it is probably necessary that the microfluidic device be composed of a reduced ratio of PDMS and an increased ratio of gas impermeable materials such as parylene or glass. However, it would be ideal that despite integration with gas impermeable materials that the microfluidic device would be compatible with the described Braille-based pumping and valving system because with Braille, the capabilities are already in place for dynamic switching from recirculation to perfusion culture to model ischemia-reperfusion injury in a manner not possible with conventional model systems.

One of the strengths of microfluidic systems is the ability to recreate physiological conditions more faithfully than conventional static-based systems.[16] However, an underlying limitation of current microfluidic systems is the lack of integration of readily quantifiable and biologically meaningful measurement capabilities.[2, 17] For instance, the biological measurements that were made within microfluidic devices that were described in this dissertation were changes in cell morphology (Chapter II), cell survival (Chapter III), and cell adhesion (Chapter IV). Although these measurements provided invaluable insight with regard to their respective studies, these measurements on

their own are not capable of elucidating the molecular mechanisms occurring either intracellularly or extracellularly that are of great importance in understanding the underlying biology. In order for cell-based microfluidic systems to be more widely adopted by cell biologists, these systems must not only integrate rudimentary biological measurements and assays but the commonly used molecular-based measurements and assays in a user-friendly manner. This particular problem is not a simple one to answer but is of such great importance to our field that it should be addressed with time, effort, and ingenuity. Once microfluidics becomes widely adopted by cell biologists, the volume of meaningful biological information obtained using microfluidic systems will be sure to increase dramatically.

The goals of future work that would build off the research presented in this dissertation could be focused in five different directions: 1) enhanced parallelization for increased throughput, 2) improved materials and fabrication processes, 3) escalated biological complexity to more faithfully model *in vivo* conditions, 4) improved integration of biological assays on chip, and 5) improved user-friendliness for biologists and clinicians to support translatable research. These five directions are not mutually exclusive of each other and can be investigated in combination with each other. If given the opportunity to directly advance the research presented in this dissertation, I would probably focus on directions 3) and 4). This dissertation research has focused primarily in designing and validating new platforms for studying vascular biology. It would be enjoyable to implement these platforms to advance the understanding of certain biological processes which can be accomplished once increasing both the biological

complexity and the ability to measure biology in these systems. Furthermore, successful implementation of directions 3) and 4) would strongly help validate the utility of microfluidic systems to biologists and potentially help them in the development of their own research.

Collectively, the results presented in this dissertation confirm that microfluidic technology can be used to properly mimic a broad range of the endothelial cell environments seen in physiology that may govern certain vascular diseases. Microfluidic systems possess the capabilities of precise fluid actuation,[18] formation of independent cellular compartments for parallel experiments,[19] and spatial control and delivery of biomolecules.[20] The work in this dissertation describes integration of these unique features of microfluidic systems and adapting them for endothelial cell culture. By doing so, we establish that microfluidic systems have the capabilities of advancing the understanding of endothelial cell biology as it relates to vascular diseases.

References

1. Walker, G. M.; Zeringue, H. C.; Beebe, D. J., Microenvironment design considerations for cellular scale studies. *Lab on a Chip* **2004,** 4, (2), 91-97.

2. El-Ali, J.; Sorger, P. K.; Jensen, K. F., Cells on chips. *Nature* **2006,** 442, (7101), 403-411.

3. Song, J. W.; Gu, W.; Futai, N.; Warner, K. A.; Nor, J. E.; Takayama, S., Computer-controlled microcirculatory support system for endothelial cell culture and shearing. *Analytical Chemistry* **2005,** 77, (13), 3993-3999.

4. Davies, P. F., FLOW-MEDIATED ENDOTHELIAL MECHANOTRANSDUCTION. *Physiological Reviews* **1995,** 75, (3), 519-560.

5. Heo, Y. S.; Cabrera, L. M.; Song, J. W.; Futai, N.; Tung, Y. C.; Smith, G. D.; Takayama, S., Characterization and resolution of evaporation-mediated osmolality shifts that constrain microfluidic cell culture in poly(dimethylsiloxane) devices. *Anal Chem* **2007,** 79, (3), 1126-34.

6. Carden, D. L.; Granger, D. N., Pathophysiology of ischaemia-reperfusion injury. *J Pathol* **2000,** 190, (3), 255-66.

7. Bockhorn, M.; Jain, R. K.; Munn, L. L., Active versus passive mechanisms in metastasis: do cancer cells crawl into vessels, or are they pushed? *Lancet Oncology* **2007,** 8, (5), 444-448.

8. Ali, S.; Lazennec, G., Chemokines: novel targets for breast cancer metastasis. *Cancer and Metastasis Reviews* **2007,** 26, (3-4), 401-420.

9. Luker, K. E.; Luker, G. D., Functions of CXCL12 and CXCR4 in breast cancer. *Cancer Letters* **2006,** 238, (1), 30-41.

10. Muller, A.; Homey, B.; Soto, H.; Ge, N. F.; Catron, D.; Buchanan, M. E.; McClanahan, T.; Murphy, E.; Yuan, W.; Wagner, S. N.; Barrera, J. L.; Mohar, A.; Verastegui, E.; Zlotnik, A., Involvement of chemokine receptors in breast cancer metastasis. *Nature* **2001,** 410, (6824), 50-56.

11. Phillips, R. J.; Burdick, M. D.; Lutz, M.; Belperio, J. A.; Keane, M. P.; Strieter, R. M., The stromal derived factor-1/CXCL12-CXC chemokine receptor 4 biological axis in non-small cell lung cancer metastases. *Am J Respir Crit Care Med* **2003,** 167, (12), 1676-86.

12. Khamsi, R., Labs on a chip Meet the stripped down rat. *Nature* **2005,** 435, (7038), 12-13.

13. Freedman, D. H., The silicon guinea pig. *Technology Review* **2004,** 107, (5), 62-+.

14. Fisher, A. B.; Chien, S.; Barakat, A. I.; Nerem, R. M., Endothelial cellular response to altered shear stress. *American Journal of Physiology-Lung Cellular and Molecular Physiology* **2001,** 281, (3), L529-L533.

15. Mehta, G.; Mehta, K.; Sud, D.; Song, J. W.; Bersano-Begey, T.; Futai, N.; Heo, Y. S.; Mycek, M. A.; Linderman, J. J.; Takayama, S., Quantitative measurement and control of oxygen levels in microfluidic poly(dimethylsiloxane) bioreactors during cell culture. *Biomed Microdevices* **2007,** 9, (2), 123-34.

16. Walker, G. M.; Zeringue, H. C.; Beebe, D. J., Microenvironment design considerations for cellular scale studies. *Lab Chip* **2004,** 4, (2), 91-7.

17. Blow, N., Microfluidics: in search of a killer application. *Nat Meth* **2007,** 4, (8), 665-670.

18. Unger, M. A.; Chou, H. P.; Thorsen, T.; Scherer, A.; Quake, S. R., Monolithic microfabricated valves and pumps by multilayer soft lithography. *Science* **2000,** 288, (5463), 113-6.

19. Gu, W.; Zhu, X.; Futai, N.; Cho, B. S.; Takayama, S., Computerized microfluidic cell culture using elastomeric channels and Braille displays. *Proc Natl Acad Sci U S A* **2004,** 101, (45), 15861-6.

20. Takayama, S.; Ostuni, E.; LeDuc, P.; Naruse, K.; Ingber, D. E.; Whitesides, G. M., Subcellular positioning of small molecules. *Nature* **2001,** 411, (6841), 1016.